FINAL REPORT
OFFICE OF NAVAL RESEARCH
Contract No. N00014-86-K-0255

PHENOMENOLOGICAL STUDIES IN MICROMECHANICS

D. Post, and R. Czarnek
Virginia Polytechnic Insitute and State University
Engineering Science and Mechanics Department
Blacksburg, Virginia 24061

September, 1988

TABLE OF CONTENTS

EXECUTIVE SUMMARY

State of the art experimental techniques have been applied to micromechanical measurements of advanced composite materials and structures.

Moire interferometry has been used to determine the phenomenological nature of deformation of thick graphite epoxy laminates, and to measure representative mechanical properties. These properties include Young's modulus, Poisson's ratios, shear moduli and co-efficients of thermal expansion.

Test methods used for the measurement of shear moduli have been evaluated and a new test configuration proposed.

The photomechanics experiments uncovered and quantified edge effects which were also studied in detail numerically. The practical nature of stresses, which are held in some circles to be singular, was investigated and the scale over which these effects act was determined. It would appear that a very fine scale and extremely high local stress gradients occur.

A micromechanical analysis of metal-matrix specimens revealed highly anomalous deformations.

A series of experiments has been performed to determine the magnitude and distribution of residual stresses in thick composites. The experiments were particularly successful in uncovering higly localized residual tensile and shear strain concentrations.

Many of the experimental observations were made possible by the expansion of laboratory facilities which were completed towards the middle of this reporting period. This expansion has allowed significant developments in the techniques of high sensitivity strain measurement.

Improvements in grating quality have been achieved and applied to composite mechanics investigations. Experiments have been taken off the optical table and performed on a universal testing machine. A two stage process to yield an almost ten-fold increase in sensitivity has been investigated; preliminary results are exciting. This method will allow further penetration into the micromechanics domain in composite materials. Complementing this research, significant progress toward achieving zero-thickness gratings has been made.

A very active research group which includes three faculty and seven Ph.D. students has been established and many research papers are in preparation.

SIGNIFICANT RESULTS AND MAJOR ACCOMPLISHMENTS

(i) Interlaminar shear moduli of thick composite laminates have been determined. Surprisingly high localized strains have been identified between plies.

(ii) Edge effect stresses have been isolated and quantified. Remarkable variations (from lamina to lamina interface) have been observed. The scales over which the edge stress predominate have been determined and shown to be, in some cases, extremely small. Large, and possibly singular, stresses have been measured at bimaterial interfaces.

(iii) Residual strains have been measured to a sensitivity sufficient to pick up the major steps in the composite fabrication method and possible errors in the stacking sequence identified. Very large tensile strains were revealed in interlaminar zones.

(iv) Major improvements in experimental technique have been accomplished. A new method of grating production has greatly improved the quality of the experimentally determined displacement contours and extended the range of deformation measurement. Pilot experiments have already achieved sensitivities approaching the equivalent of moire with 500,000 lines per inch. Zero-thickness gratings have been prepared, but further reserach is needed for routine implementation.

RESEARCH THRUSTS

Interlaminar Shear Behavior of Thick Composites

With the primary objective of determining the shear moduli, interlaminar shear specimens were cut from thick composite tubes as shown in Fig. 1. Two types of rail shear configurations, illustrated in Fig. 2., were evaluated. Typical fringe patterns for the shear-loaded composite are presented in Fig. 3. Shear strain distributions, along and across the specimen, were obtained from these displacement data. Such shear strain distributions are shown in Figs. 4 and 5. The latter figure indicates the presence of large shear strain gradients between plies and peak shear strains in these regions of about double mean values. The large variations of performance of nominally equivalent plies (Fig. 5) documents a very important phenomenological feature. The presence of a fabrication defect is also uncovered and related to the composite microstructure in Fig. 5.

An objective of this study was to obtain material property data. In this experiment, representative values of interlaminar shear moduli (G_{13}, G_{23}) were obtained. These are summarized in Table 1.

Determination of shear properties led to consideration of other possible test configuratins. It should be noted that there is no universally accepted test method. The Iosipescu (v-notch) specimen was first evaluated. Typical fringe patterns obtained by moire interferometry are shown in Fig. 6. The patterns indicate the presence of, very nearly, pure shear. (There is evidence of bending effects from the fixture).

A new test fixture (Fig. 7), which used a compact double-notched specimen, was designed and the uniformity of the shear strain fields assessed. Fig. 8 shows the displacement fields from the moire interferometry experiment with this specimen. The uniformity of the shear field is impressive, Fig. 9a, and the new test fixture looks most promising. Figure 9b shows results for in-plne shear of the thick-walled cylinder (Fig. 1); the stress-strain relationship is nonlinear right from the start. Important attributes of this new method of measuring in-plane shear properties include economy of material (allowing use of specimens cut from curved bodies) and specimen preparation, the test can be carried out on a wide range of materials on a variety of testing machines and the test section is unaffected by the clamping. Both in-plane and interlaminar shear behavior can be determined with this specimen configuration.

Interlaminar Compression

Experiments upon cubes cut from the thick composite cylinders allowed the determination of the interlaminar modulus of elasticity and the Poisson's ratio as well as a detailed study of the phenomenological behavior. The latter gave rise to an analysis of edge effects in this

specimen.

a. Material Properties

The general specimen configuration and relationship to the original cylinder are shown in Fig. 10. Moire interferometry was used to obtain the in-plane components of displacement on the faces A and B of the cube - Figs. 11 and 12. A related experiment utilizing a Twyman - Green Interferometer provided the out-of-plane displacement component in the form of the fringe contours shown in Fig. 13. The need for this complementary experiment became apparent when the y-displacement field (Fig. 12) showed surprising differences in nominally similar plies. It was then essential to determine whether or not the phenomenon was a surface effect or indicative of bulk material behavior. The out-of-plane deformation suggested the presence of local (line) edge effects between the 0 and 90 deg plies. Thus, average values for the mechanical properties had to be calculated. These were obtained as follows:

$$E_{ave} = \frac{P/A}{\varepsilon_{yave}} = 1.4 \times 10^6 \text{ psi}$$

$$\nu_A = \frac{\bar{\varepsilon}_{xA}}{\bar{\varepsilon}_{yA}} = 0.13 \text{ and } \nu_B = \frac{\bar{\varepsilon}_{zb}}{\bar{\varepsilon}_{yB}} = 0.06$$

where subscript A or B refers to the face on which measurements were made and the bar notation indicates an average value across the specimen width.

b. Edge Stresses

Detailed studies of the edges of the specimen in Fig. 11 indicate the presence of high (corner) edge effect shear stresses. These are shown on an expanded scale in Fig. 14 which also provides an

illustration of the shear strain distribution near the edge and between two plies. Perhaps most important of all, it was discovered that the peak values of these shear strains varied from interface to interface with a factor of up to two difference. That is, nominally identical interfaces suffered significant differences in shear.

c. Interface Problem

The sensitivity and resolution of the interlaminar compression experiment were not sufficient to allow a detailed study of the nature of the high edge stresses. To gain insight into this, the behavior of a bimaterial joint (analagous to the junction between two plies of differing orientation) has been studied in detail. Experiments have been performed on brass and steel plates silver-soldered together and having the dimensions shown in Fig. 15. High frequency gratings were replicated at various locations at a temperature of 240°F above ambient. (The grating on a ULE [ultra low expansion] glass allowed a precise knowledge of the initial grating frequency.) The deformation fields associated with the mismatch in the thermo-mechanical properties of the steel and brass were recorded using moire and Twyman-Green interferometers. A typical fringe pattern is shown in Fig. 16. Abrupt changes are apparent at the material interface. The addition of appropriate carrier patterns for the steel and brass effectively substract the (uniform) thermal strains and highlight the mechanical. The results of this technique are shown in Fig. 17. Such fringe patterns allow direct calculation of the thermally induced stresses from a knowledge of the elastic constants. A typical stress distribution is presented in Fig. 18 for the quarter-point, i.e., for the line that crosses the interface 1/4 the interface length from the edge. It

appears at first glance that equilibrium of the normal stress across the interface is violated. A numerical study of the problem was performed using finite element analysis. A full three dimensional model was required to show that extremely close to the interface the stress in the brass turns upwards toward the value in the steel. While the stress gradients are very large, σ_y equilibrium is not violated. Both experiment and calculation indicate the presence of a "skin" of non-uniform stress around the interface. This is further illustrated in Fig. 19 which shows that the depth of the skin may be significant at least under the influence of a double singularity at a corner. This study is continuing with further experiment and comparison with detailed calculations to determine the practical aspects of the theoretical singularities at such interfaces.

Residual Strain Measurements

a. Thermal Strains

The residual thermal strains in a cube specimen cut from the thick composite cylinder - Fig. 20 - were measured using the same technique as in the bimetallic interface experiment. The photomechnics experiments provided the fringe patterns shown in Fig. 21 which exhibited similar micromechanical edge effects to those in the interlaminar compression measurements. Details of the peak shear strains on the faces of the cube are shown in Fig. 22.

In addition to the significant edge effect of Fig. 22, the following residual deformations and co-efficients of thermal expansion were determined for cooling the laminate from its 250°F cure temperature to 76°F room temperature:

Coefficients of thermal expansion: $\alpha_x = 3.00 \times 10^{-6}$ /°F

$\alpha_y = 39.5 \times 10^{-6}$ /°F

$\alpha_z = 1.01 \times 10^{-6}$ /°F

Residual Strains: $\varepsilon_x = -520 \times 10^{-6}$

$\varepsilon_y = -6840 \times 10^{-6}$

$\varepsilon_z = -175 \times 10^{-6}$

Surface Deformation: Face A: $\Delta W = 0\text{-}9$ μm

Face B: $\Delta W = 1.5$ μm

b. Residual Mechanical Strains

Residual strains were also measured on ring specimens cut from the thick cylinder. Gratings and strain gages were applied to rings at the locations shown in Fig. 23. The ring was cut through and the deformation fields and strains relieved by the cut were determined. Values and fringe patterns are shown in Fig. 24. Additional cuts were made to relieve other residual strains. The cutting patterns and fringe contours are shown in Figs. 25 and 26. Reduction of the experimental data provided the strain distributions shown in Fig. 27. The anomalous peaks in the shear strains coincide with halts in the fabrication process, i.e., with positions of intermediate curing and errors in the stacking sequence. The anomolous peaks in ε_x reveal very large radial interlaminar tensile strains that can contribute to premature delamination.

Edge Effects in Composites

Several of the experiments mentioned above highlighted documented composite edge effects. A program is now underway with the specific objective of determining edge effects at and on a cut-out in a thick composite panel loaded in compression. The specimen geometries for this series of experiments are shown in Fig. 28. Novel features of this program include loading on a universal testing machine (that is, the experiment was moved off the optical table) and the design of a miniature interferometer to allow interrogation of the boundary surface of the hole. A detail of the interferometer is shown in Fig. 29.

The current status of the program is that the first measurements are now being taken.

Metal Matrix Investigation

A continuation of previous work on boron/aluminum laminates in the form of tensile specimens with a central slot revealed significant micromechanical characteristics. Figure 30 shows the displacments parallel to the fiber direction in the outer 45° ply of the specimen, and Fig. 31 shows the fiber-by-fiber shear strain distribution along line L3. Groups of fibers experience slip relative to neighboring groups, as highlighted by shading in Fig. 30. Strong intra-fiber slip occurs at random locations, as shown in Fig. 31. Large interlaminar shears must accompany these outer fiber displacements. Significant information on the coupling between 0° and 45° plies was revealed.

Improvement of Experimental Technique

The photomechanics experiments performed in this program have uniquely high sensitivity and produce fringe patterns of an extremely high quality. These features are a direct result of the gratings used in the experiments. Efforts have been made to improve upon these already high quality gratings. The production technique has been modified through the use of photo resist to yield gratings of optimum profile. The results of this improvement are:

- Greater diffraction efficiency which, in turn, allows shorter exposure times.
- Much higher signal-to-noise ratios (a consequence of the unique interferometer designed to provide the optimum gratings) which increases the fringe contract and the limit of the largest deformations which can be resolved before the fringes "run together".

These gratings were used in many of the experiments described above and contribute to the excellent fringe patterns. A further milestone in the development of moire interferometry was the use of a zero-thickness grating in measurements on a pin-loaded plate. For this the gratings were etched into the surface to avoid shear lag associated with the replicated (epoxy) gratings normally used.

The current practical sensitivity of moire interferometry is about 60,000 lines per inch with an optical limit of about 100,000 lines per inch. Micromechanical measurements require an ever increasing sensitivity. Two-stage methods of achieving a sensitivity corresponding to about 500,000 lines per inch are now under scrutiny. Preliminary results are encouraging and a factor of eight improvement has already been attained, as displayed in Fig. 32.

The photomechanics experiments provide vast amounts of data in the form of displacement contours. However, strains and stresses are often required. The reduction of the experimental data can be tedious. As a first step in the automation of this process, a localized hybrid method of data reduction has been developed. This consists of using the photomechanics displacement data as boundary conditions in a finite element analysis of an arbitrary region of interest. Detailed studies have shown that the high sensitivity of moire interferometry is required for meaningful analyses; excellent results have been obtained in investigations of frictional contact phenomena in pin-loaded metallic and composite plates.

Summary of Research Progress

Optical techniques have been used to measure composite properties, to examine and improve composite test methods and investigate fundamental mechanical phenomena in composites, especially thick composites. The nature of edge effects has received much attention. Studies of interlaminar shear, in-plane shear, interlaminar compression, residual thermal strains, residul mechanical strains, and interface problems are reported. Graphite/epoxy and boron/aluminum specimens were investigated.

In parallel with these studies improvements have been made in the techniques themselves. These will allow higher sensitivity measurements to be made on a micromechanics level.

Numerous technical publications have evolved from this end closely related work, as listed in Sections (i-k) herein. Others are being prepared. Some seven papers have been submitted for presentation at the

forthcoming SEM meeting in Boston next June.

The basic objectives of the sponsored research -- investigation of phenomenological behavior in micromechanics and enhancement of techniques for finer-scale measurements -- have been achieved.

LIST OF PUBLICATIONS

1. D. Post, "Moire Interferometry," Chap. 7, Handbook of Experimental Mechanics, A. S. Kobayashi, Editor, Prentice-Hall, Englewood Cliffs, NJ (1987).

2. D. Post, R. Czarnek, D. Joh, J. Jo and Y. Guo, "Experimental Study of a Metal-Matrix Composite," Experimental Mechanics, 27(2), pp. 190-194 (June 1987).

3. D. Post, R. Czarnek, D. Joh, J. Jo and Y. Guo, "Deformation of a Metal-Matrix Tensile Coupon with a Central Slot: an Experimental Study," Jl. of Composites Technology and Research (ASTM), Vol. 9, No. 1, pp. 3-9 (Spring 1987).

4. K. Patorski, D. Post, R. Czarnek and Y. Guo, "Real-Time Optical Differentiation for Moire Interferometry," Applied Optics, Vol. 26, pp. 1977-1982 (May 14, 1987).

5. D. Post, K. Patorski and P. Ning, "A Compact Grating Interferometer for Producing Photoresist Gratings with Incoherent Light," Applied Optics, Vol. 26, pp. 1100-1104 (Mar. 15, 1987).

6. D. Post, "The Analysis of Deformations and Strains in Composites by Moire Interferometry", Proceedings, Sixth International Conference on Composite Materials and Second European Conference on Composite Materials, F. L. Matthews, N. C. R. Buskell, J. M. Hodgkinson and J. Morton, Editors, Elsevier, NY, 1987, Vol. 5, pp. 5.251-5.261.

7. R. Czarnek, D. Post and Y. Guo, "Strain Concentration Factors in Composite Tensile Members with Central Holes," Proceedings of the 1987 SEM Spring Conference on Experimental Mechanics, Houston, TX (June 14-19, 1987).

8. Y. Guo, D. Post, R. Czarnek, "The Magic of Carrier Patterns in Moire Interferometry, SPIE Proc. Vol. 814, Bellingham, WA (In Press).

9. P. Ifju, D. Post, "Thermal Strain Analysis Using Moire Interferometry," SPIE Proc. Vol. 814, Bellingham, WA (In Press).

10. D. Joh, R. Czarnek and D. Post, "Measurements of Micro-slip Amplitude Around the Pin Joint of Plates Using Moire Interferometry," SPIE Proc. Vol. 814, Bellingham, WA (In Press).

11. D. Post, R. Czarnek, j. D. Wood and D. Joh, "Deformations and Strains in a Thick Adherend Lap Joint," ASTM Special Technical Publication 981 1988, American Society for Testing Materials, 1916 Race Street, Philadelphia, PA 19103.

12. D. Post, R. Czarnek and D. Joh, "Shear Strains in a Graphite -PEEK Beam by Moire Interferometry with Carrier Fringes," Experimental Mechanics, 27(3), pp. 246-249 (September 1987).

13. Y. Guo, D. Post and R. Czarnek, "The Magic of Carrier Patters in Moire Interferometry," Experimental Mechanics, (in press).

14. D. Post, f. L. Dai Y. Guo and P. Ifju, "Interlaminar Shear Moduli of Cross-Ply Laminates; An Experimental Analysis," Journal of Composite Materials, (in press).

15. D. Post, R. Czarnek, J. Morton, B. Han and M. Y. Tsai, "Experimental Studies of Contact Stress With Friction," ONR Contract N00014-84-K-0552 Final Report.

16. D. Post and J. D. Wood, "Determination of Thermal Strains by Moire Interferometry," Experimental Mechanics, (to be published).

17. D. Post, Y. Guo and R. Czarnek, "Deformation Analysis of Boron/Aluminum Specimens by Moire Interferometry," Journal of Composites Technology and Research, (to be published).

18. D. Post, J. McKelvie, M. Tu, and F. L. Dai, "Fabrication of Holographic Gratings using a Moving Point Source," Applied Optics (to be published).

LIST OF PARTICIPANTS

Faculty

D. Post (Professor)
J. Morton (Professor
R. Czarnek (Assistant Professor)

Visitors

F. L. Dai (Visiting Professor, Tsinghua U., Beijing, China). 1987/88
J. McKelvie (Visiting Professor, U. Strathclyde, Scotland). 1987/88
M. Tu (Visiting Scholar, Chinese Academy of Science,Beijing).1987/88.
Y. Wang (Visiting Scholar Tianjin U., Tianjin, China). 1987/88
K. Patorski (Visiting Scientist, Warsaw Technical University, Poland. 1986 (June-October)
J. Wasowski (Visiting Scientist, Warsaw Technical University, Poland. 1986 (June-December)

Graduate Research Assistants

R. Boeman (Ph.D. Student)
Y. Guo (Ph.D. Student)
B. Han (Ph.D. Student)
P. Ifju (Ph.D. Student)
J. Lee (Ph.D. Student)
M. Tsai (Ph.D. Student)
J. Wood (Ph.D. Student)

	Property	Specimen I		Specimen II	
		Average Value	Extreme Variations	Average Value	Extreme Variations
RESIN-RICH ZONE EXCLUDED	$G_0 = G_{13}$ Center of Ply [Eq. 2]	3.7 GPa 540,000 psi	+ 17% - 28%	3.6 GPa 520,000 psi	+ 11% - 14%
	$G_{90} = G_{23}$ Center of Ply [Eq. 2]	2.8 GPa 400,000 psi	+ 14% - 18%	2.6 GPa 370,000 psi	+ 20% - 16%
	$G^{calc}_{[90_2/0]_n}$ by calculation [Eq. 5]	3.0 GPa 440,000 psi		2.9 GPa 420,000 psi	
RESIN-RICH ZONE INCLUDED	$G^{eff}_{[90_2/0]_n}$ by measurements [Eq. 3]	2.6 GPa 380,000 psi		2.8 GPa 400,000 psi	
	$G^{eff}_0 = G^{eff}_{13}$ [Eq. 6]	3.2 GPa 470,000 psi	+ 17% - 28%	3.4 GPa 500,000 psi	+ 11% - 14%
	$G^{eff}_{90} = G^{eff}_{23}$ [Eq. 6]	2.4 GPa 350,000 psi	+ 14% - 18%	2.4 GPa 350,000 psi	+ 20% - 16%

TABLE I Summary of experimentally determined interlaminar shear moduli.

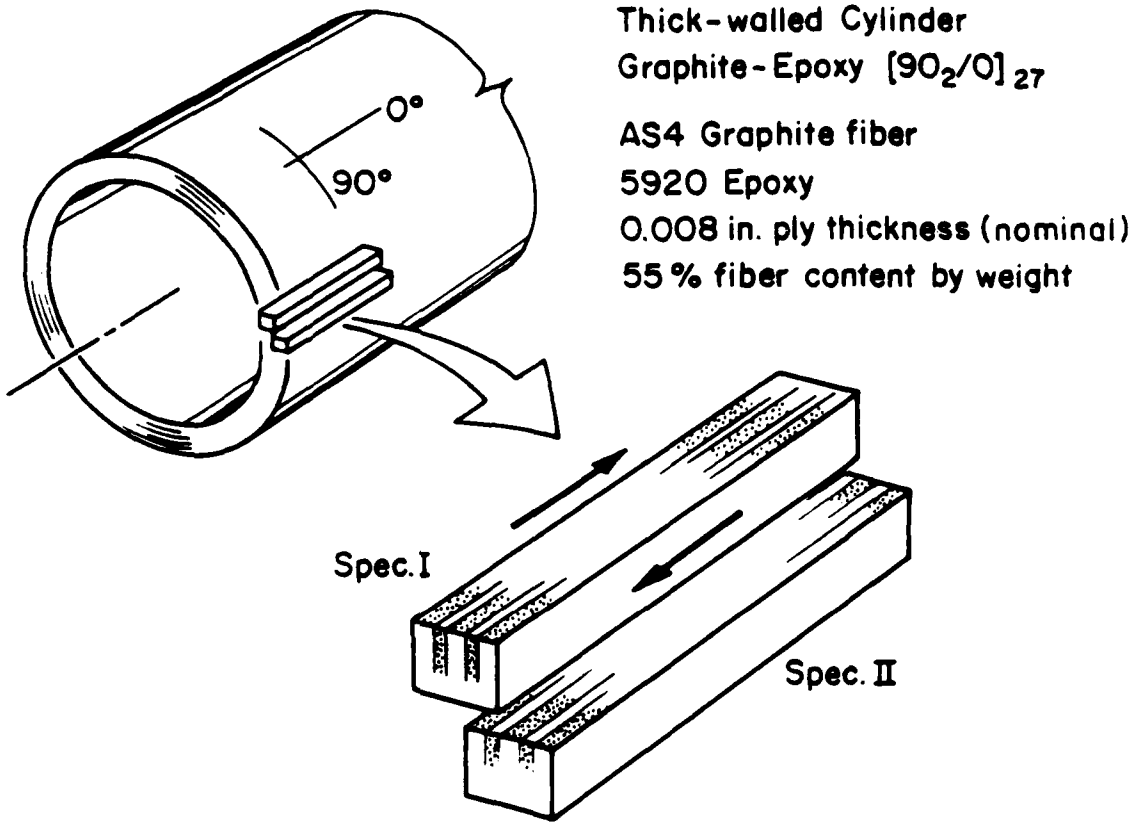

Fig. 1 Details of thick-walled composite cylinder and the specimens cut for the rail shear interlaminar shear moduli measurements.

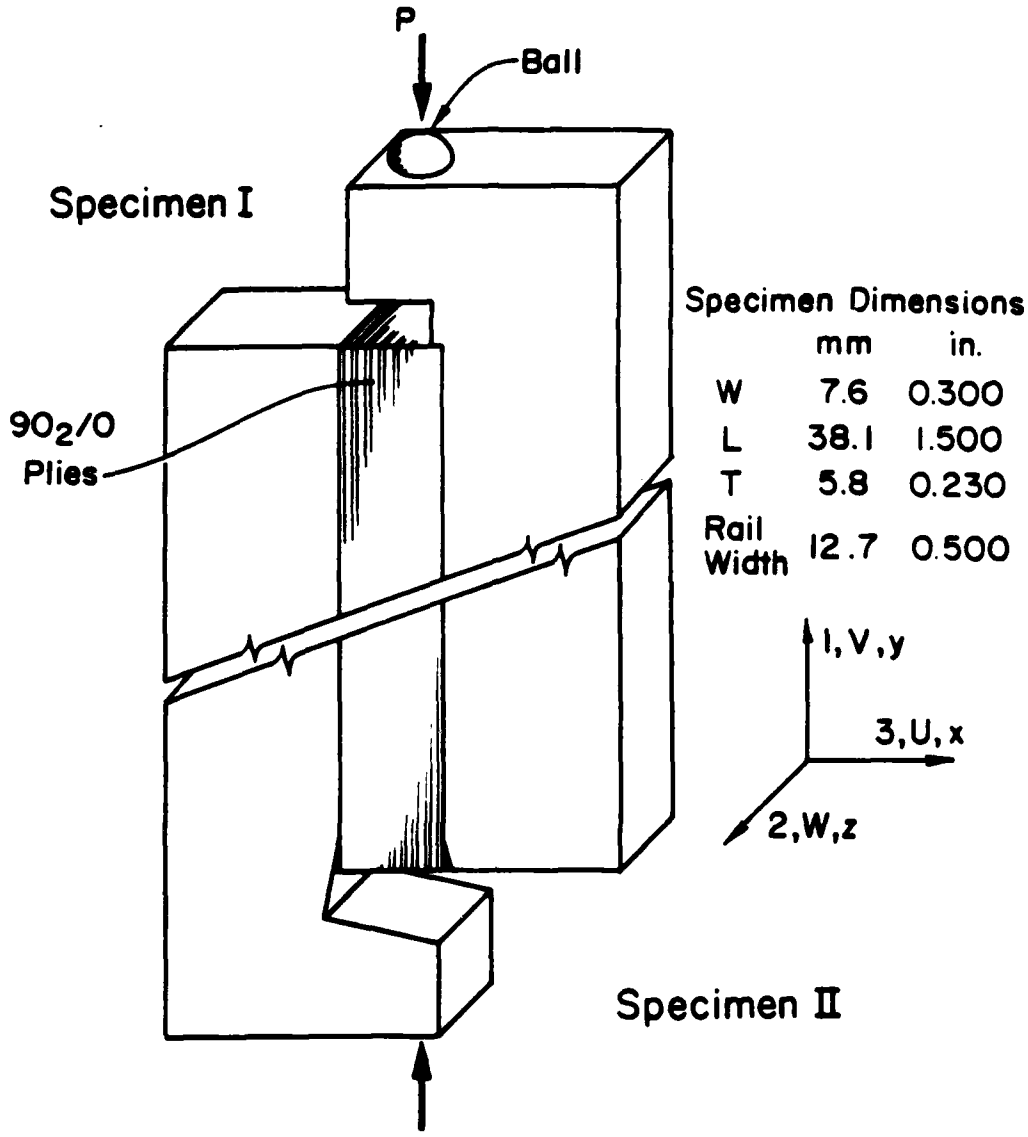

Fig. 2 Specimen configurations and dimensions for the rail shear experiments. Specimen II had a tapered cement bond at its corners. The zero deg fibers lie in the y direction.

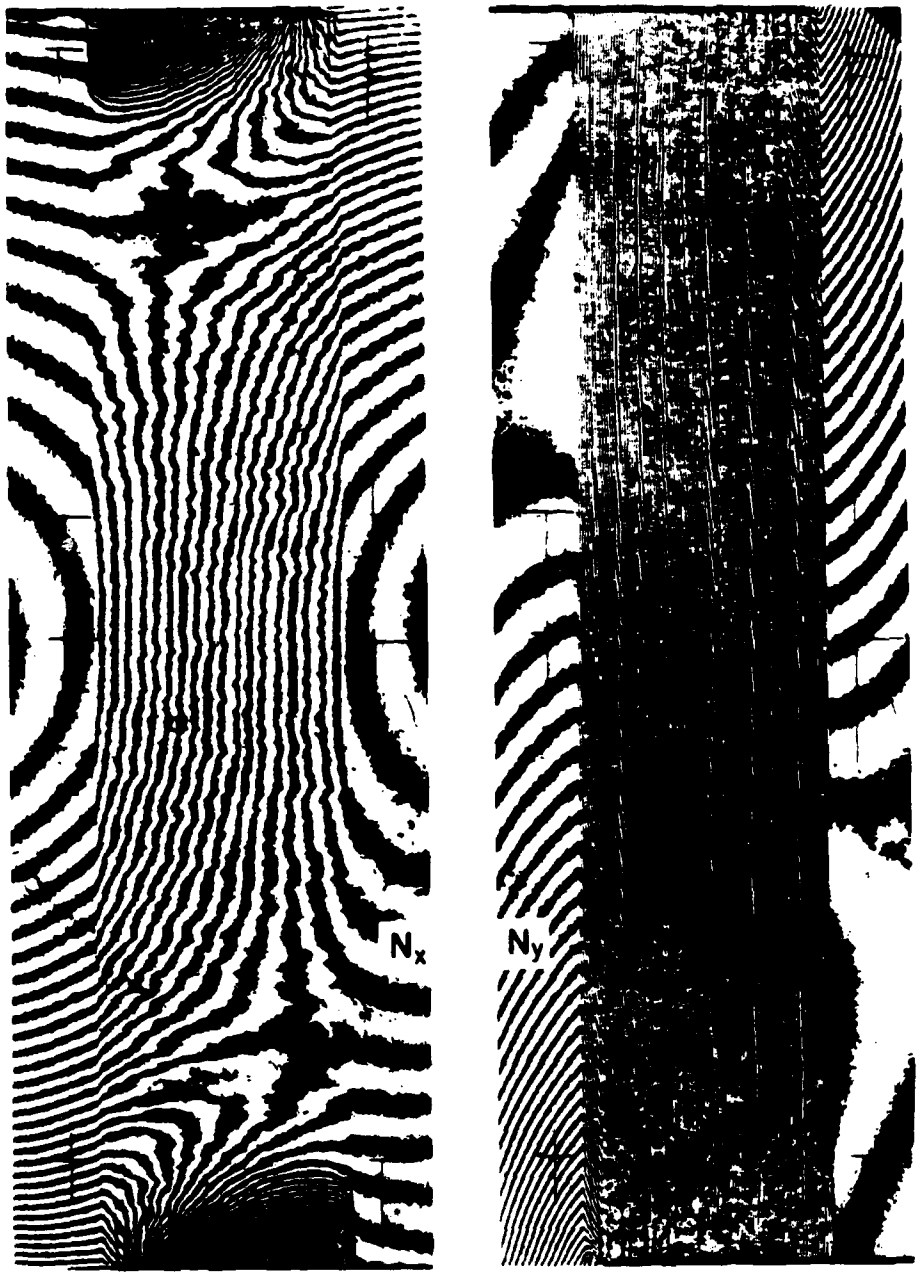

Fig. 3 Horizonal (N_x) and vertical (N_y) fringe patterns representing typical U and V displacement fields for the rail shear experiment with Specimen I. The applied load P = 3.18kN (714 lb).

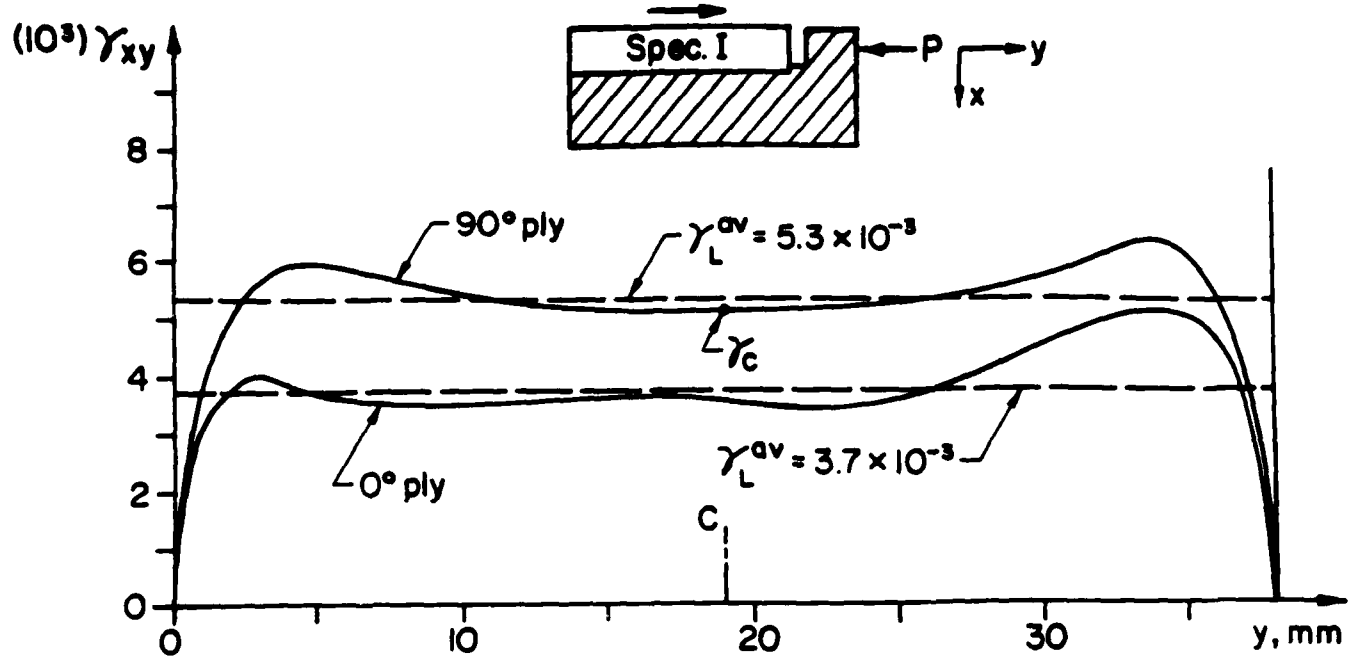

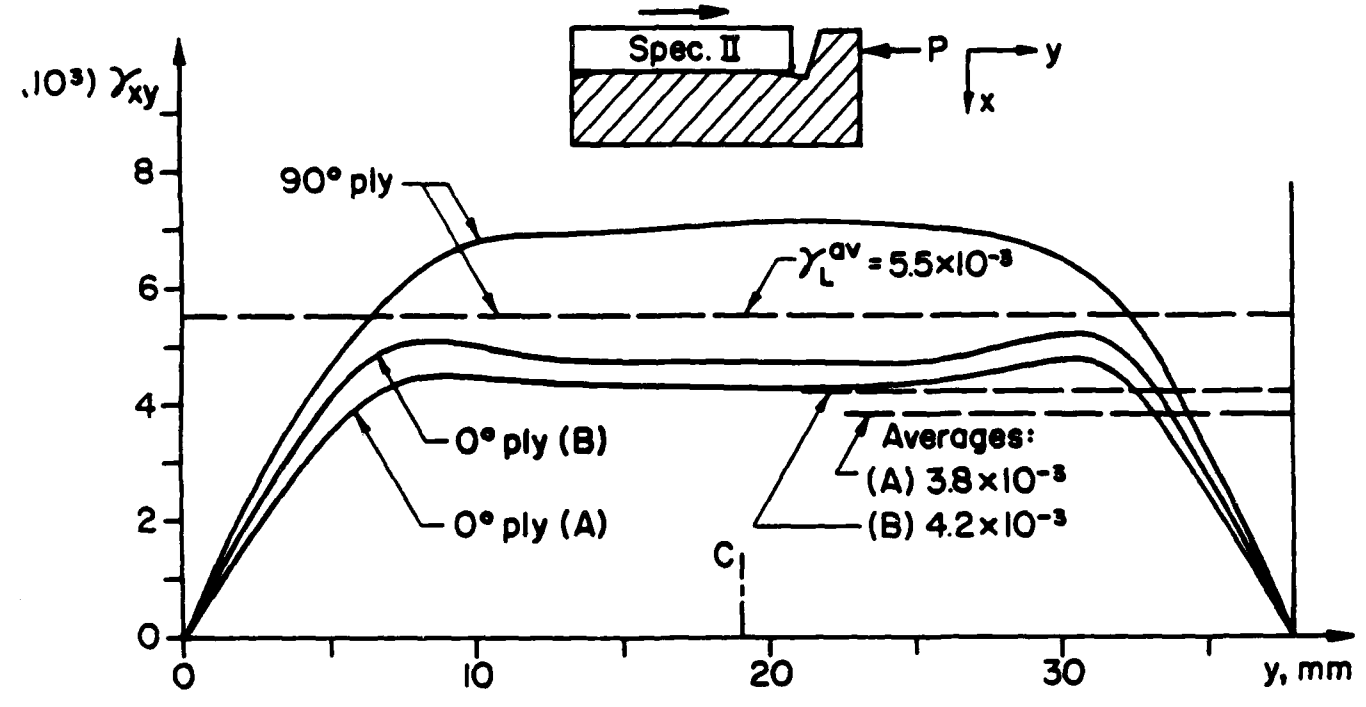

Fig. 4 Shear strain distributions along individual plies for Specimens I and II. These plies lie within the central third of the specimen.

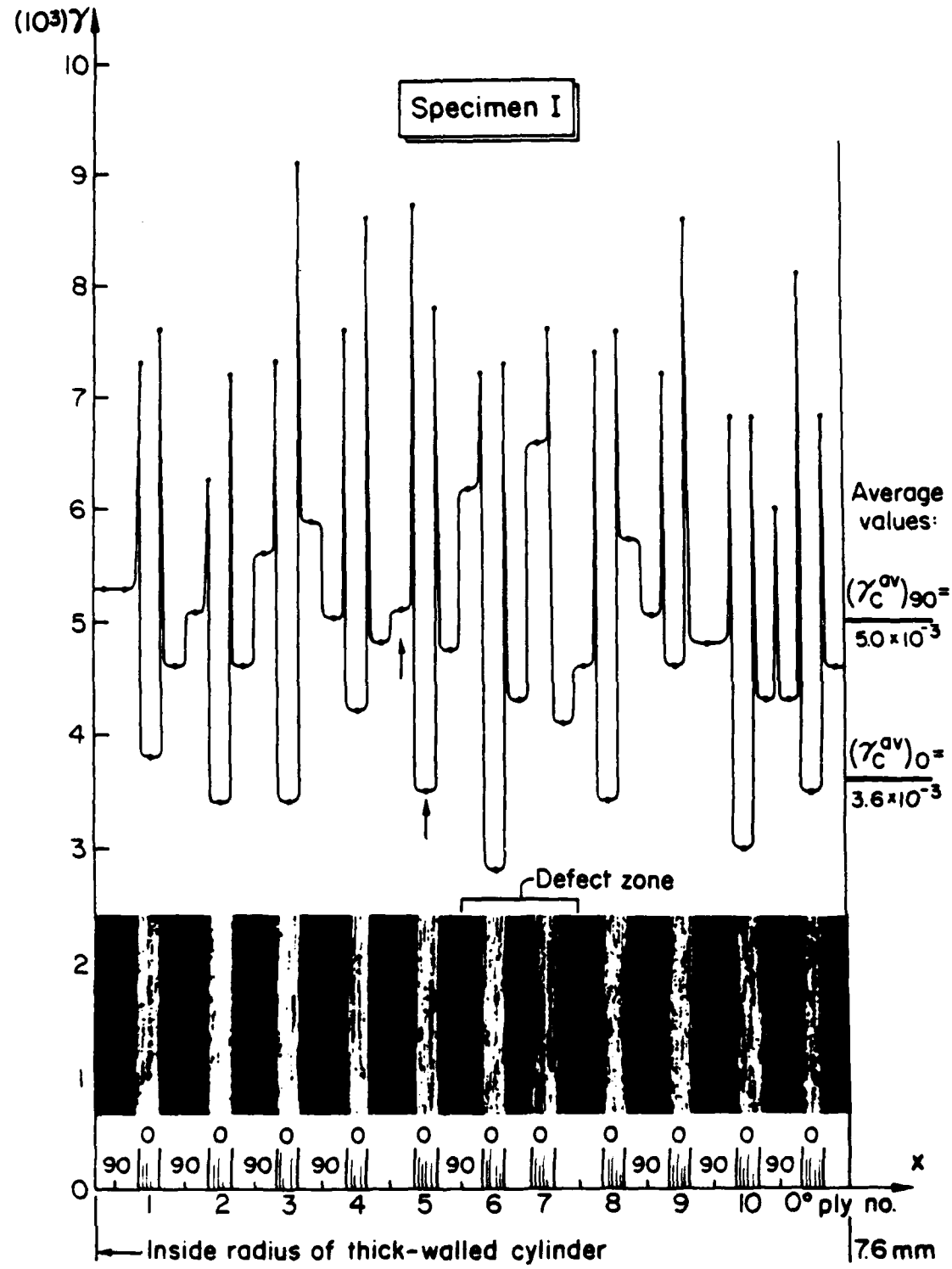

Fig. 5 Interlaminar shear strains across the width of the rail shear specimen I. Peak shear strains are apparent at the ply interfaces. The inset micrograph shows the relationship between the ply geometry and the shear strain distribution.

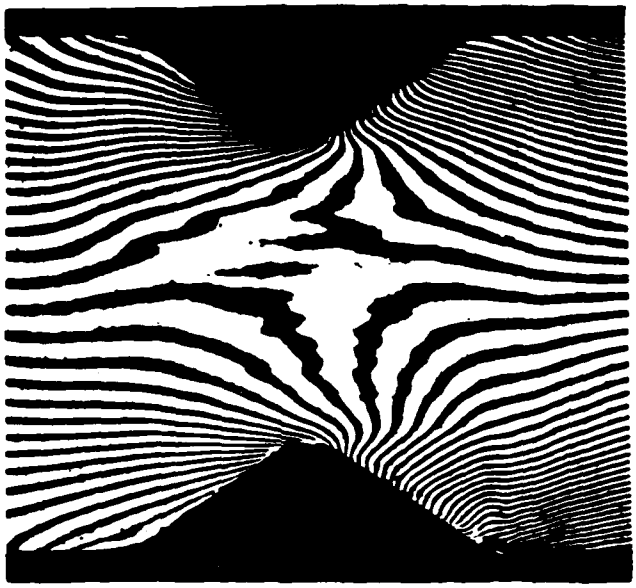

(a)

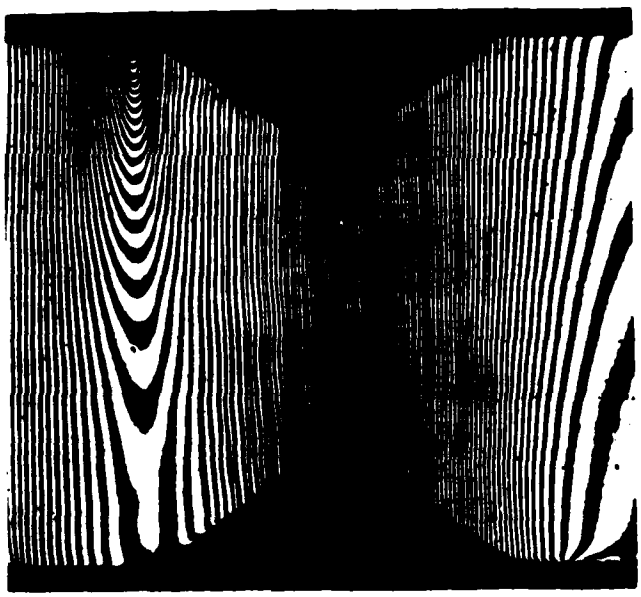

(b)

Fig. 6 Moire fringe patterns for the horizontal (a) and vertical (b) displacements in an Iosipescu specimen. These fringes correspond to very nearly pure shear in the notch section.

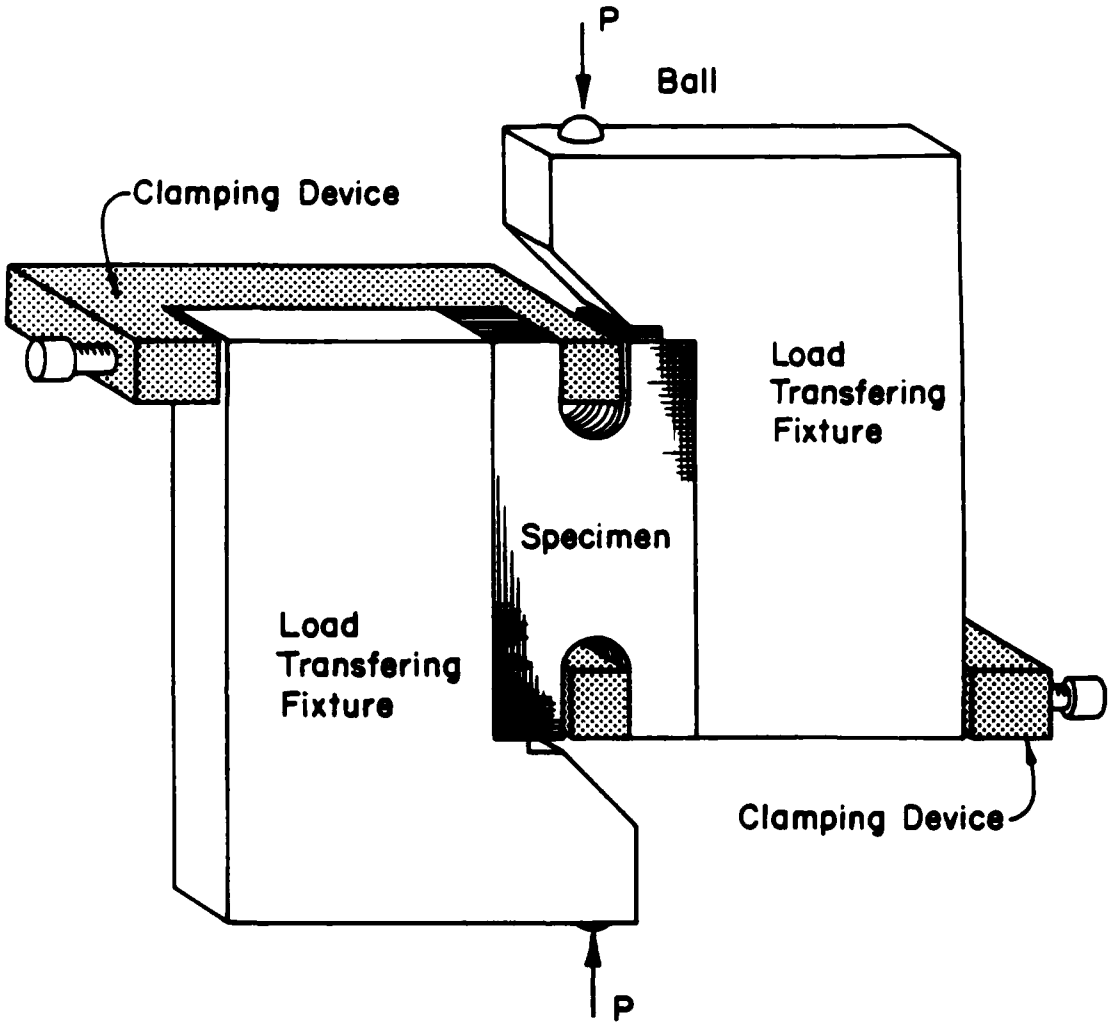

Fig. 7 General arrangement of the compact double-notched specimen for in-plane shear modulus measurement. A moire grating over the entire face of the specimen allowed shear strain measurement.

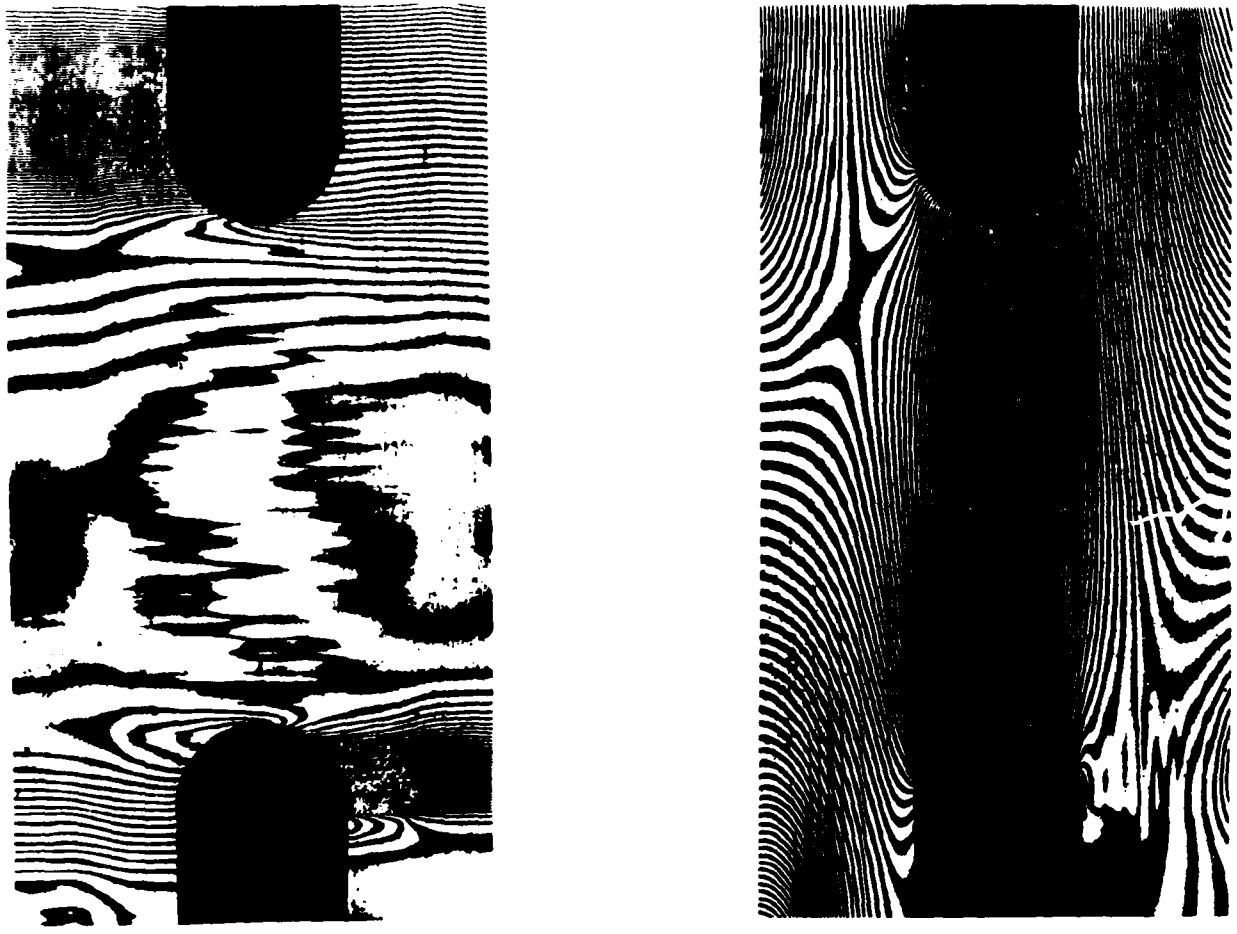

(a) (b)

Fig. 8 Moire fringe patterns for the horizontal (a) and vertical (b) displacement components for the compact double-notched shear specimen.

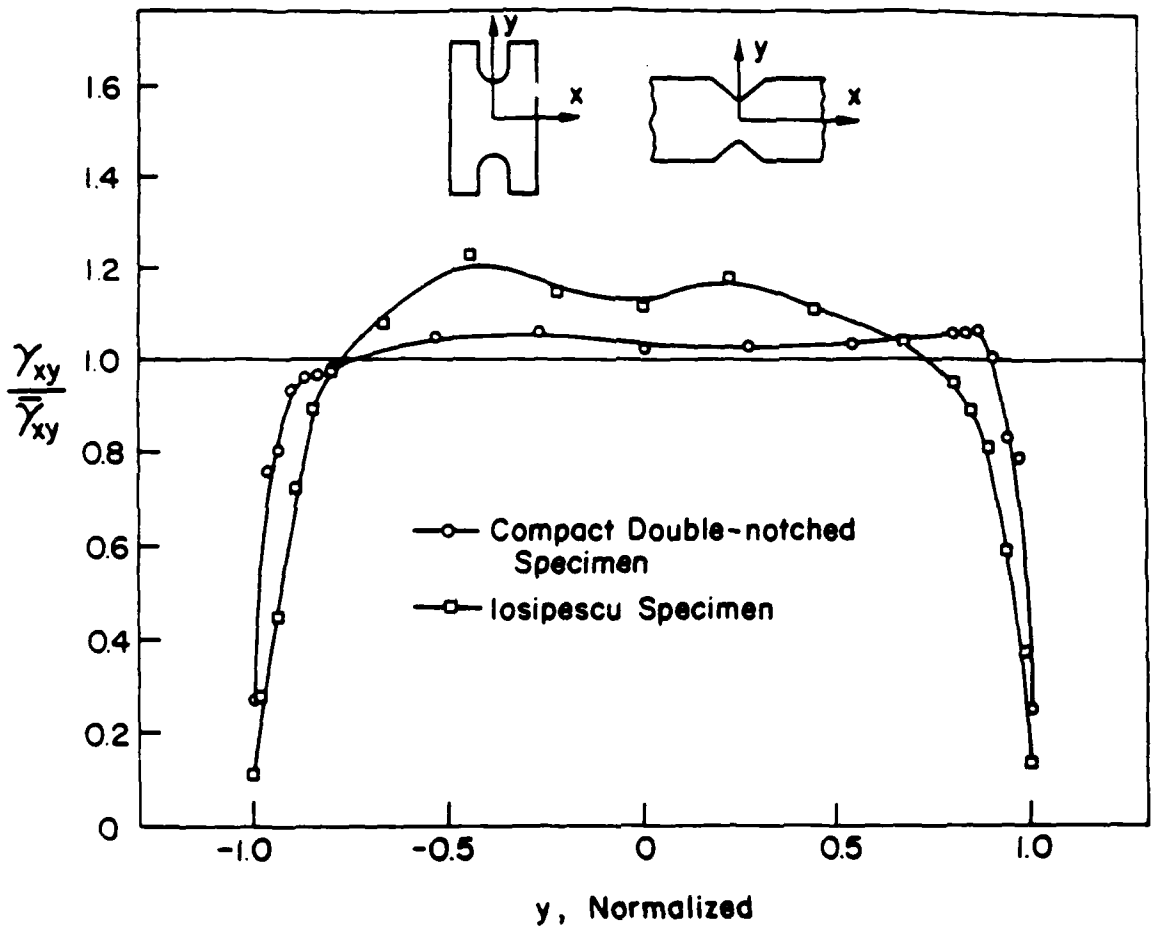

Fig. 9 (a) Shear strain distributions along a line correction the notch tips in the compact double-notched and Iosipescu specimens.

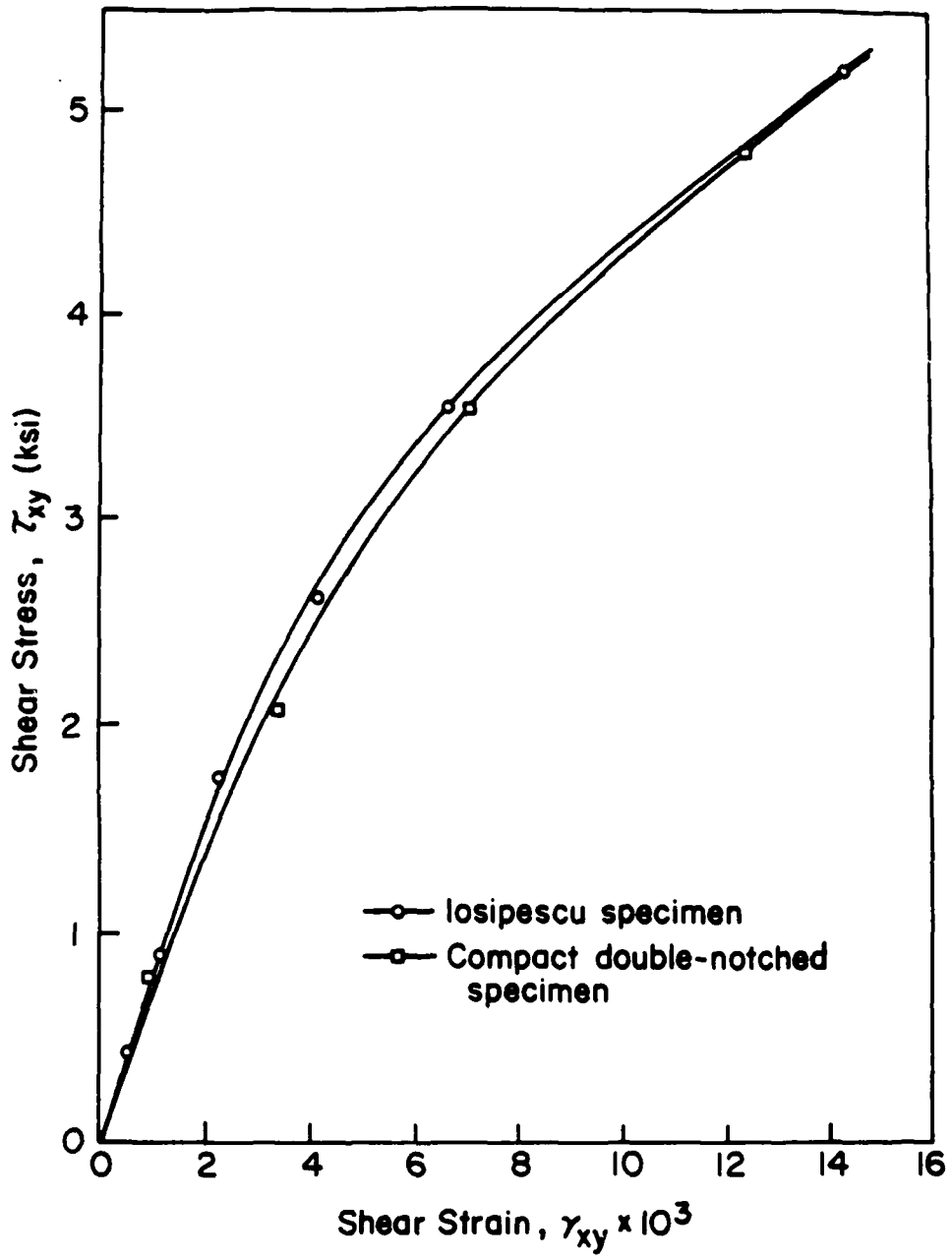

Fig. 9 (b) In-plane shear stress strain curve obtained from the compact double notched specimen. Significant non-linearity is present even at small strains.

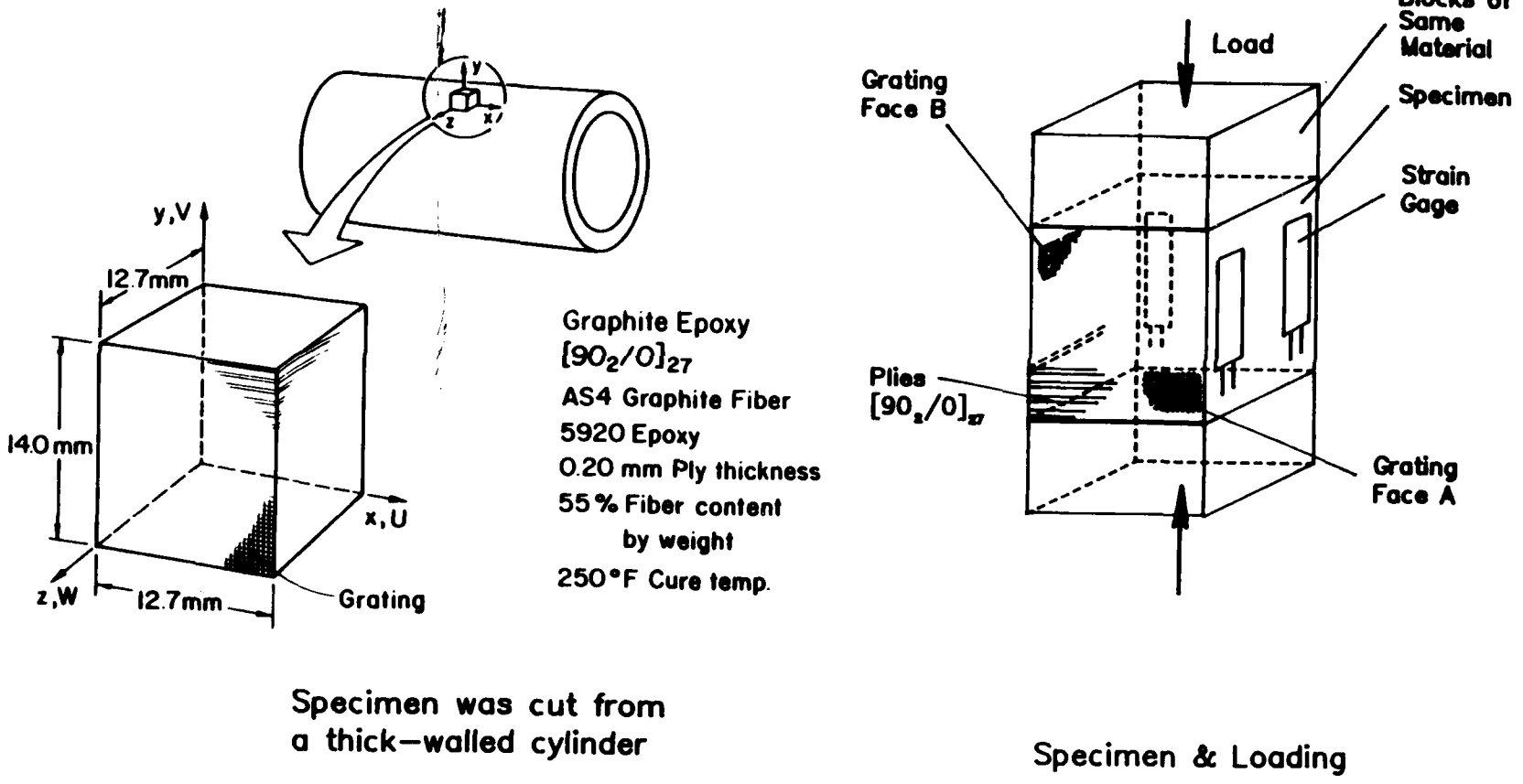

Fig. 10 Details of the interlaminar compression specimen cut from the thick composite cylinder.

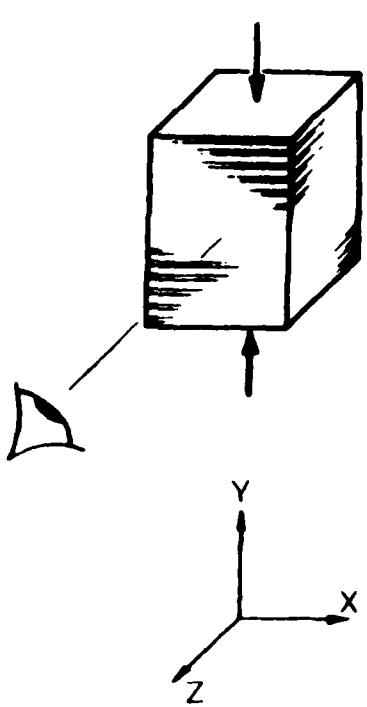

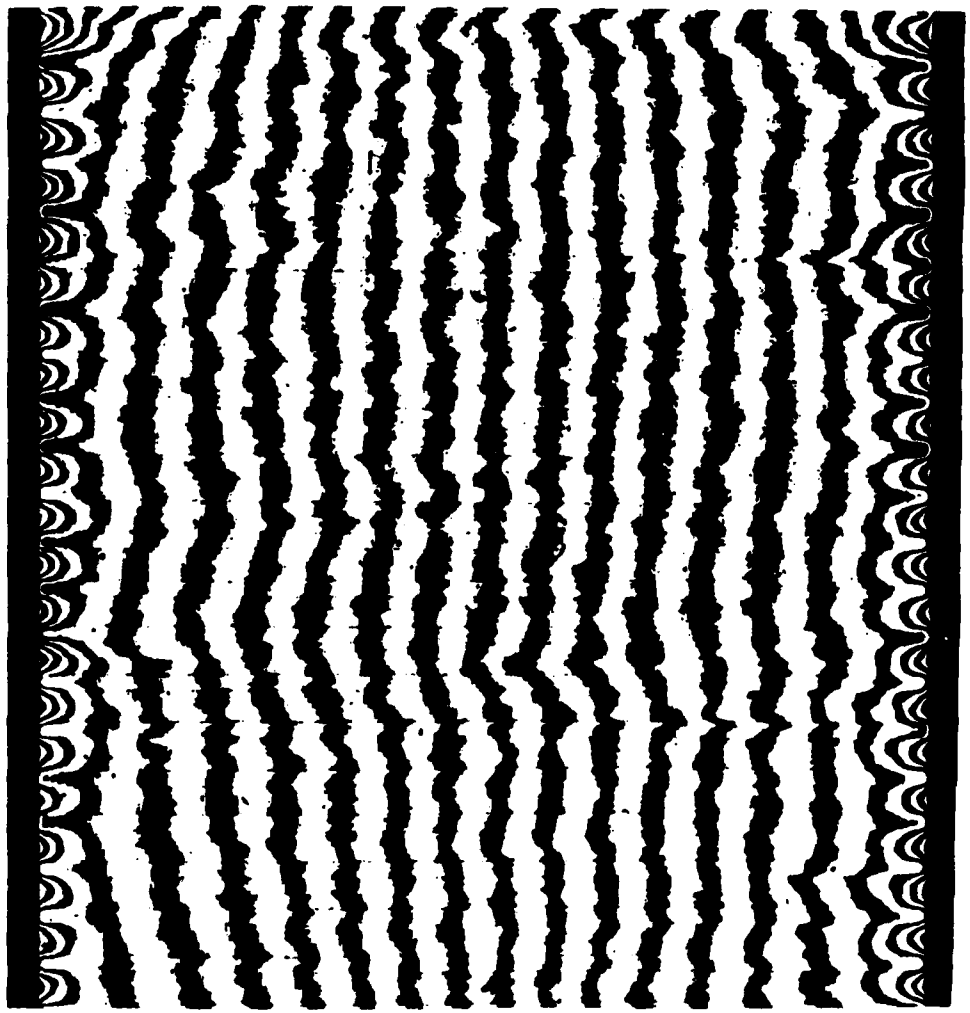

Fig. 11 Fringe pattern for the horizontal (U) component of displacement for the interlaminar compression specimen.

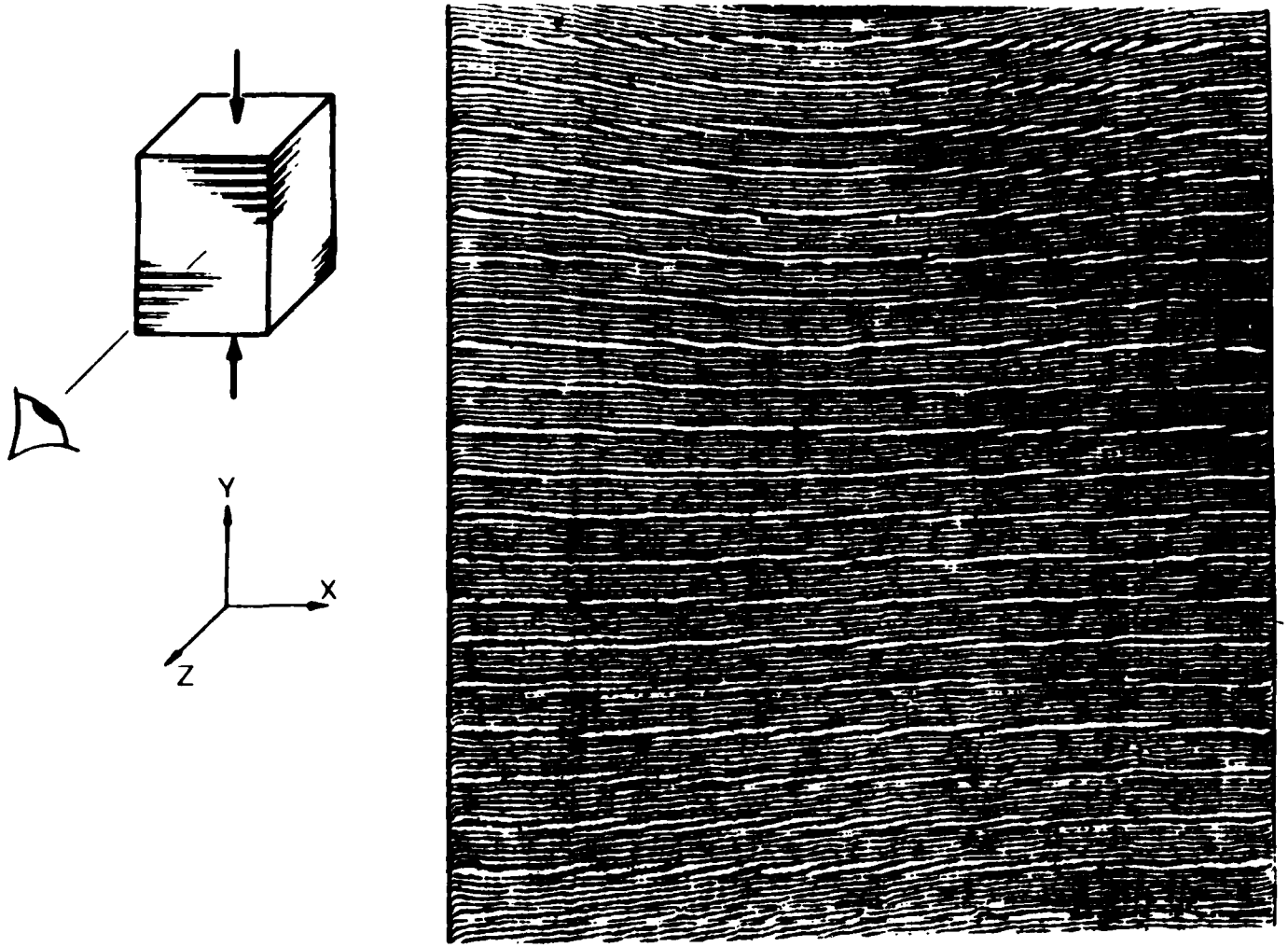

Fig. 12 Fringe pattern for the vertical (V) component of displacement for the interlaminar compression specimen.

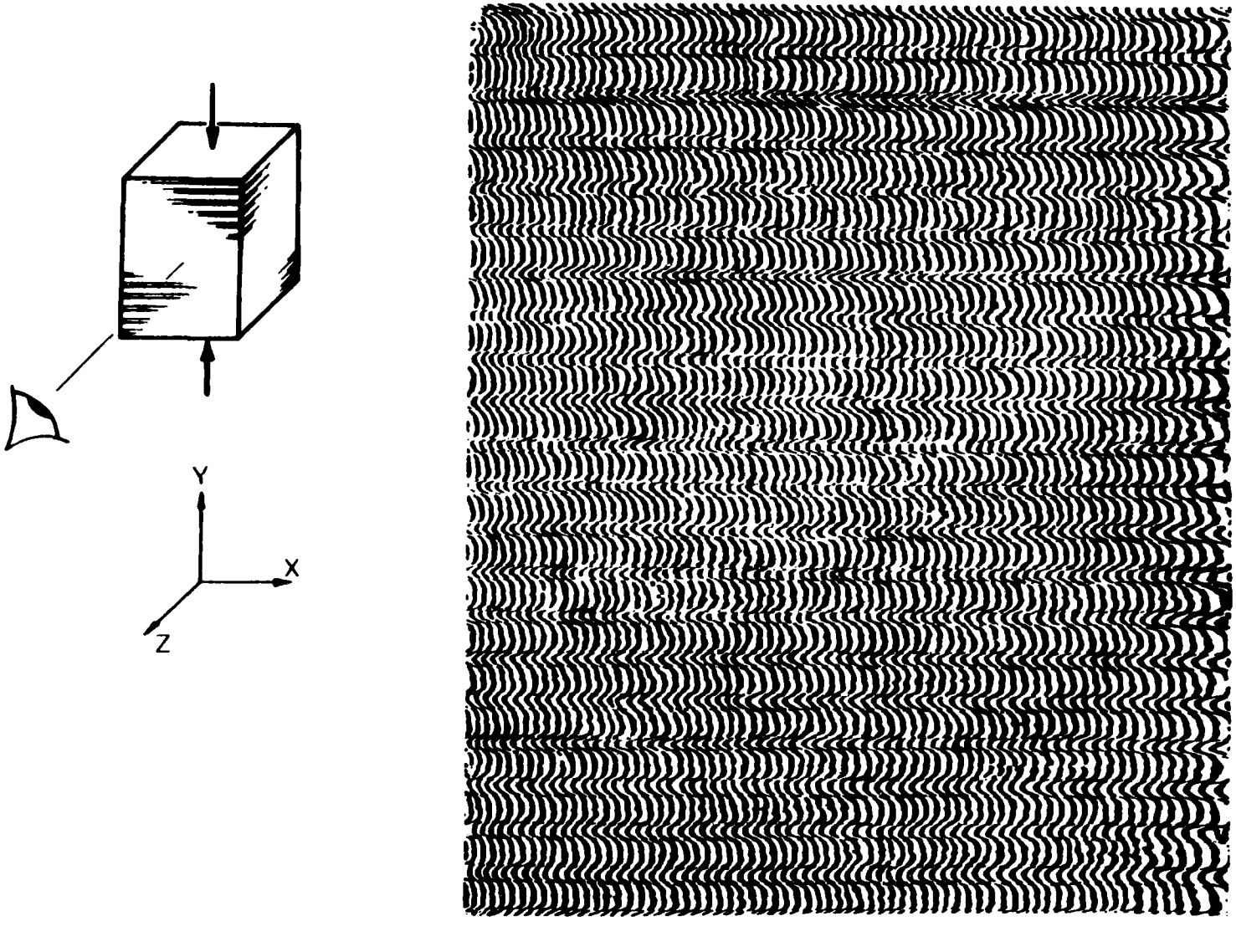

Fig. 13 Fringe pattern for the out-of-plane (W) component of displacement for the interlaminar compression specimen.

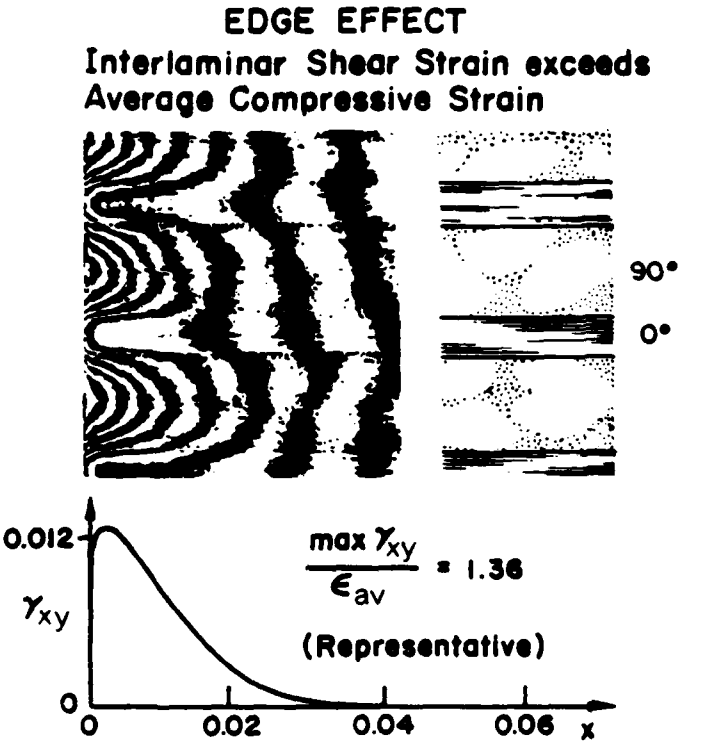

Fig. 14 Detail of free edge effect fringe pattern (U-field) and corresponding interlaminar shear strains.

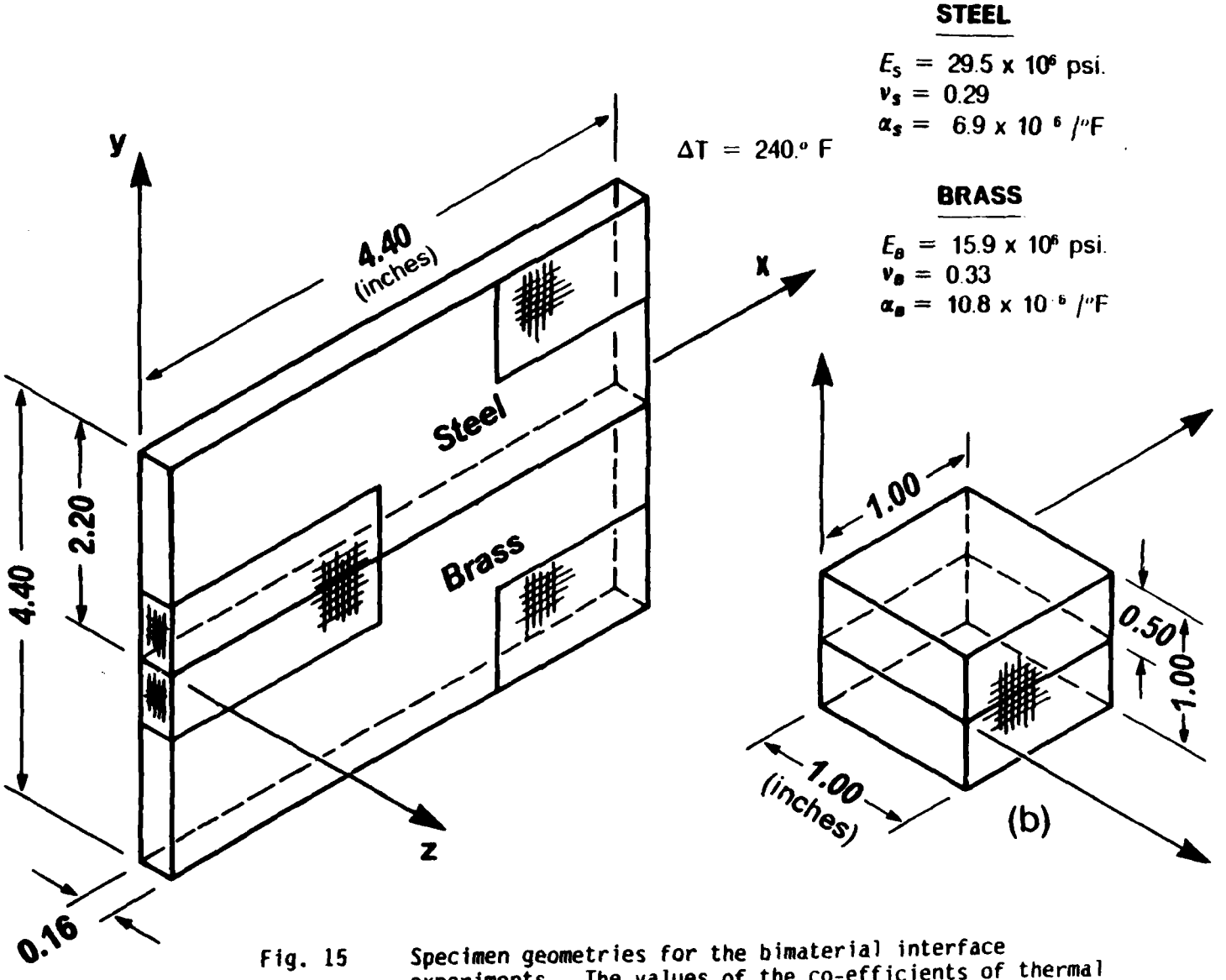

Fig. 15 Specimen geometries for the bimaterial interface experiments. The values of the co-efficients of thermal expansion (α_S and α_B) have been determined experimentally.

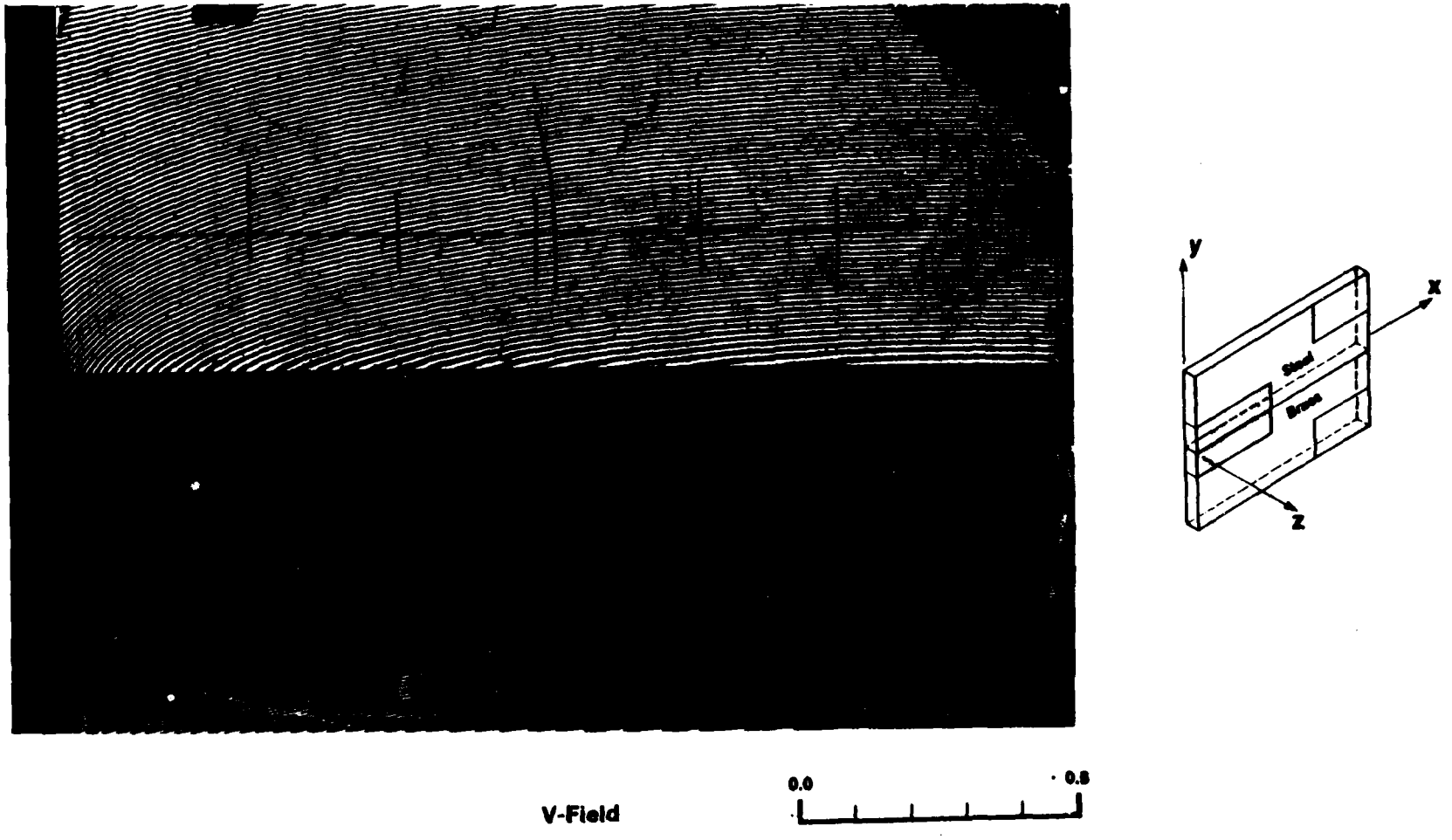

Fig. 16 A typical fringe pattern (for the vertical, V-field) near the interface at the location shown on the inset.

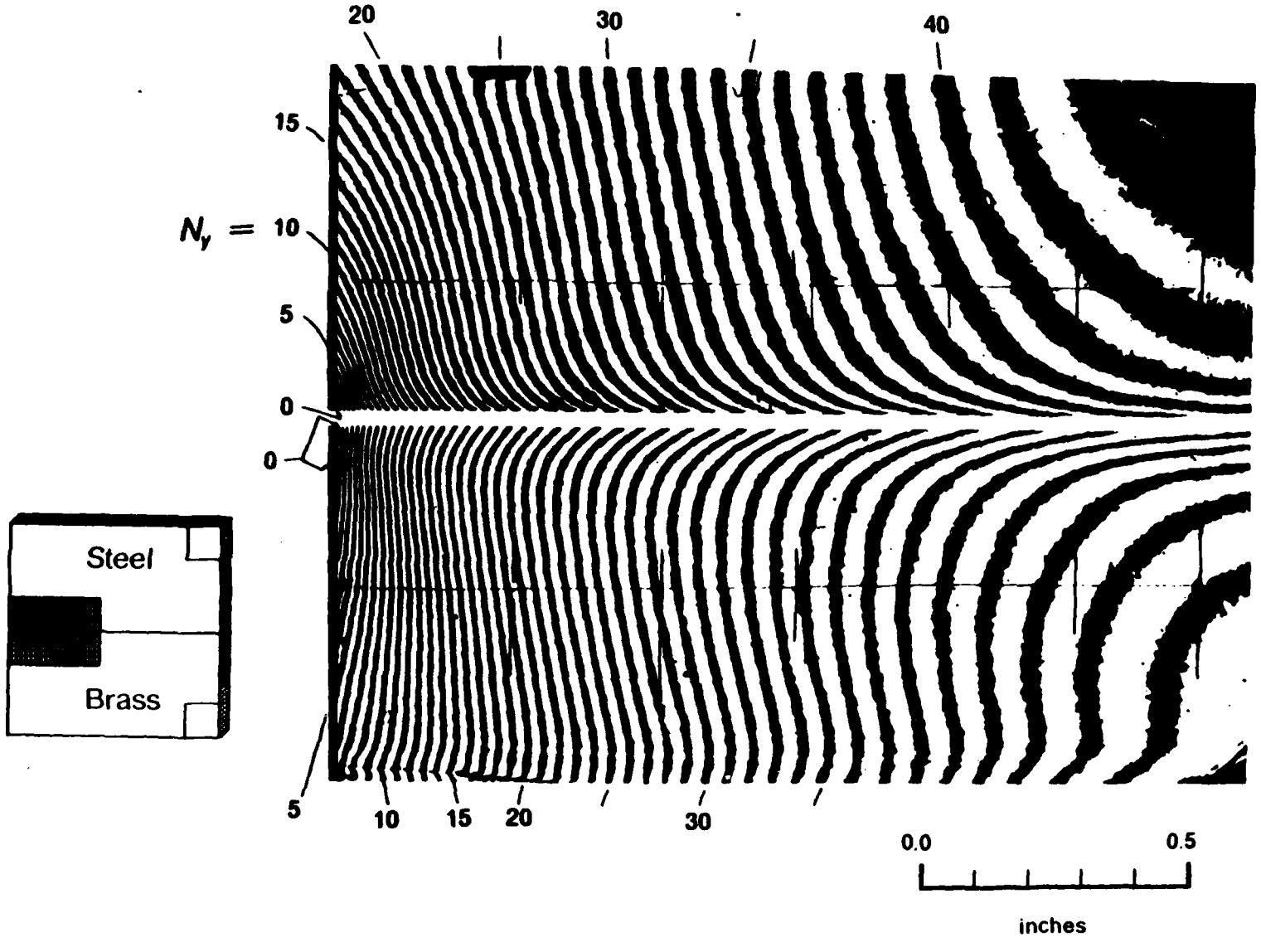

Fig. 17 Fringe patterns corresponding to mechanically induced displacements in the brass and steel. These have been obtained by optically subtracting the uniform thermal expansion.

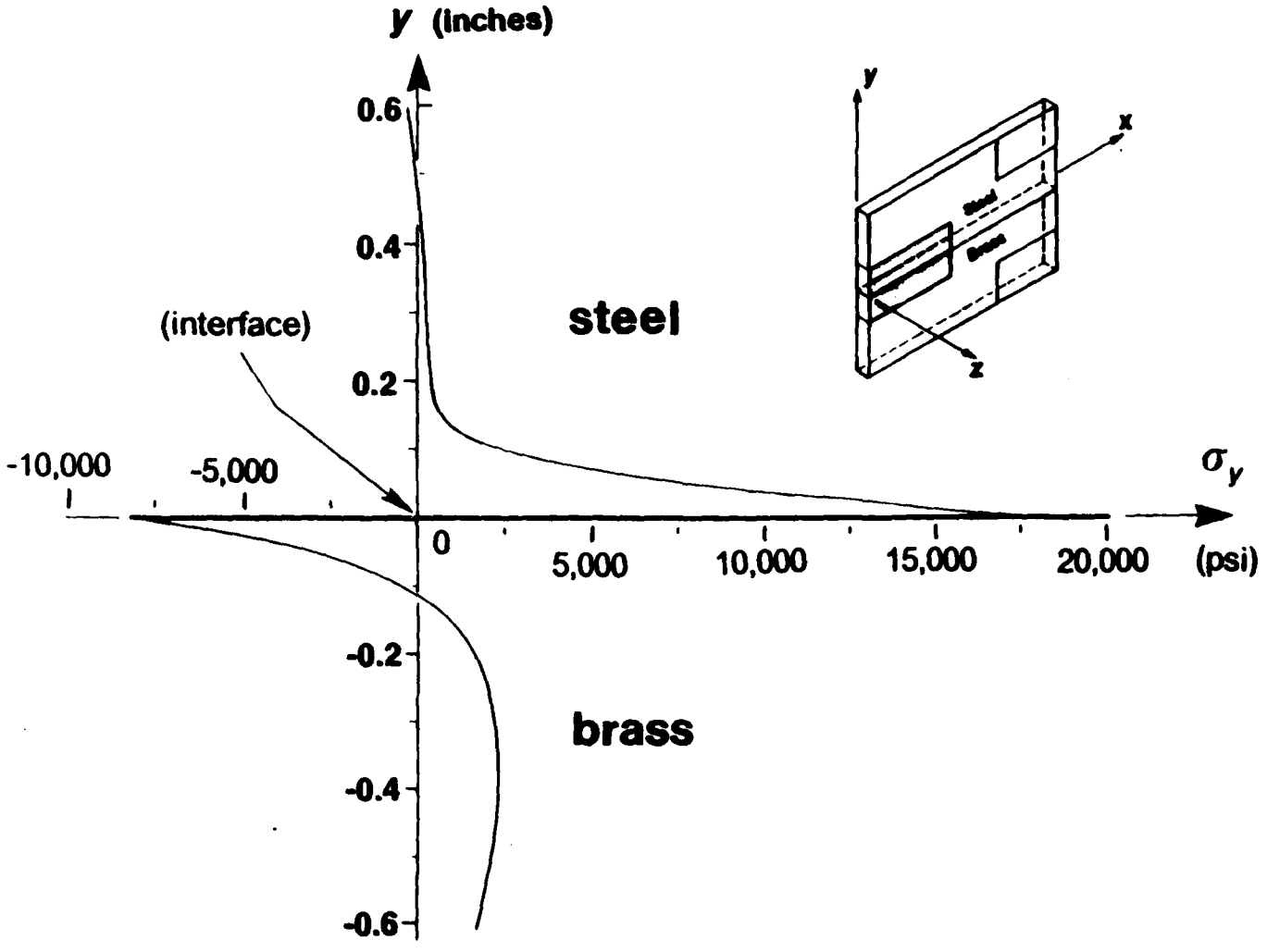

Fig. 18 Distribution of normal stress σ_y along line across the bimaterial interface. The line is located at one quarter of the length of the interface from the edge.

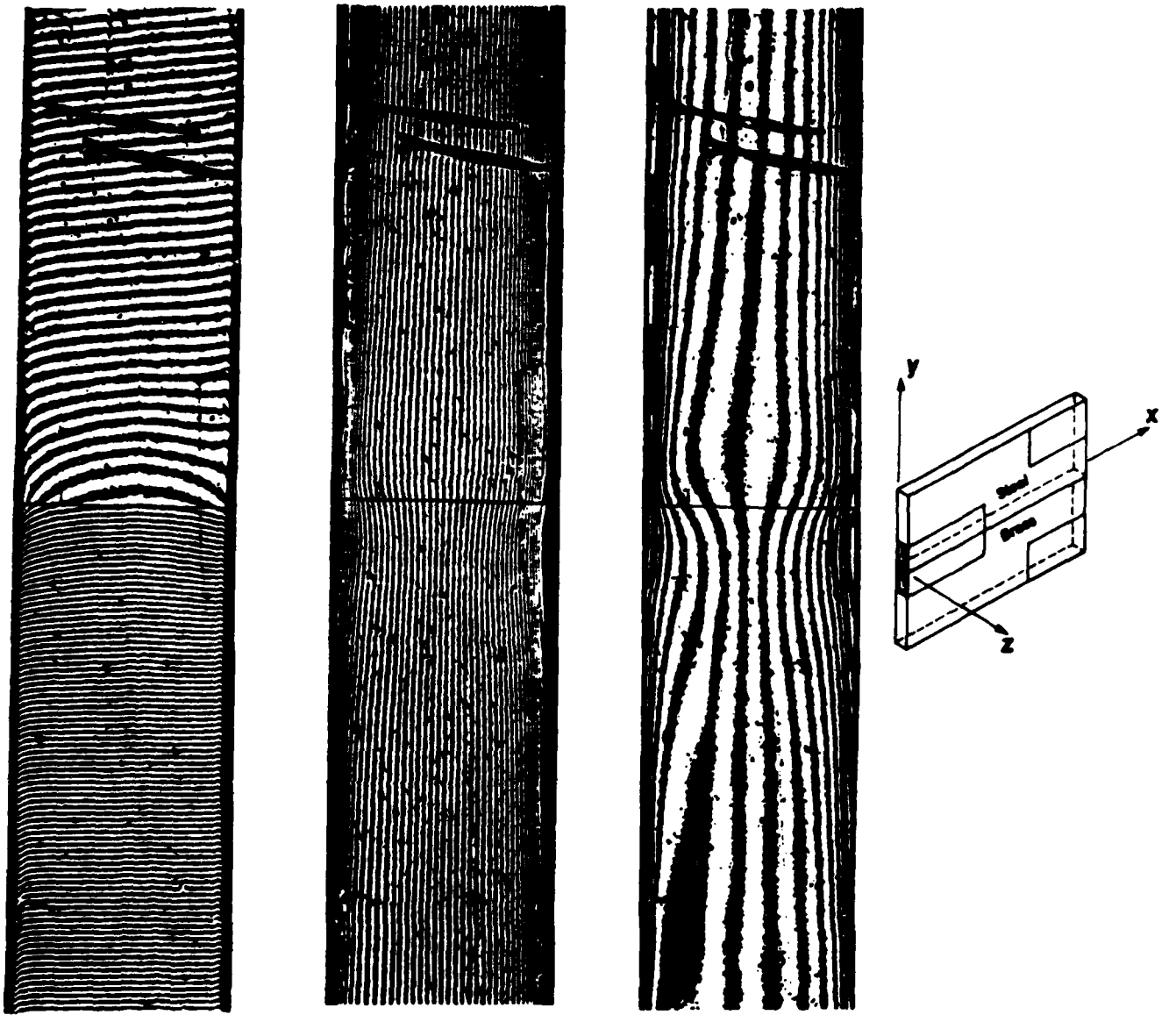

(a) V-displacement field for displacements in the y direction (no carrier added)

(b) W-displacement field for displacements in the z direction (no carrier added)

(c) W-displacement field for displacements in the z direction (with added carrier)

Fig. 19 Fringe patterns illustrating the lack of uniformity in the displacement fields caused by the (corner) free edge effects.

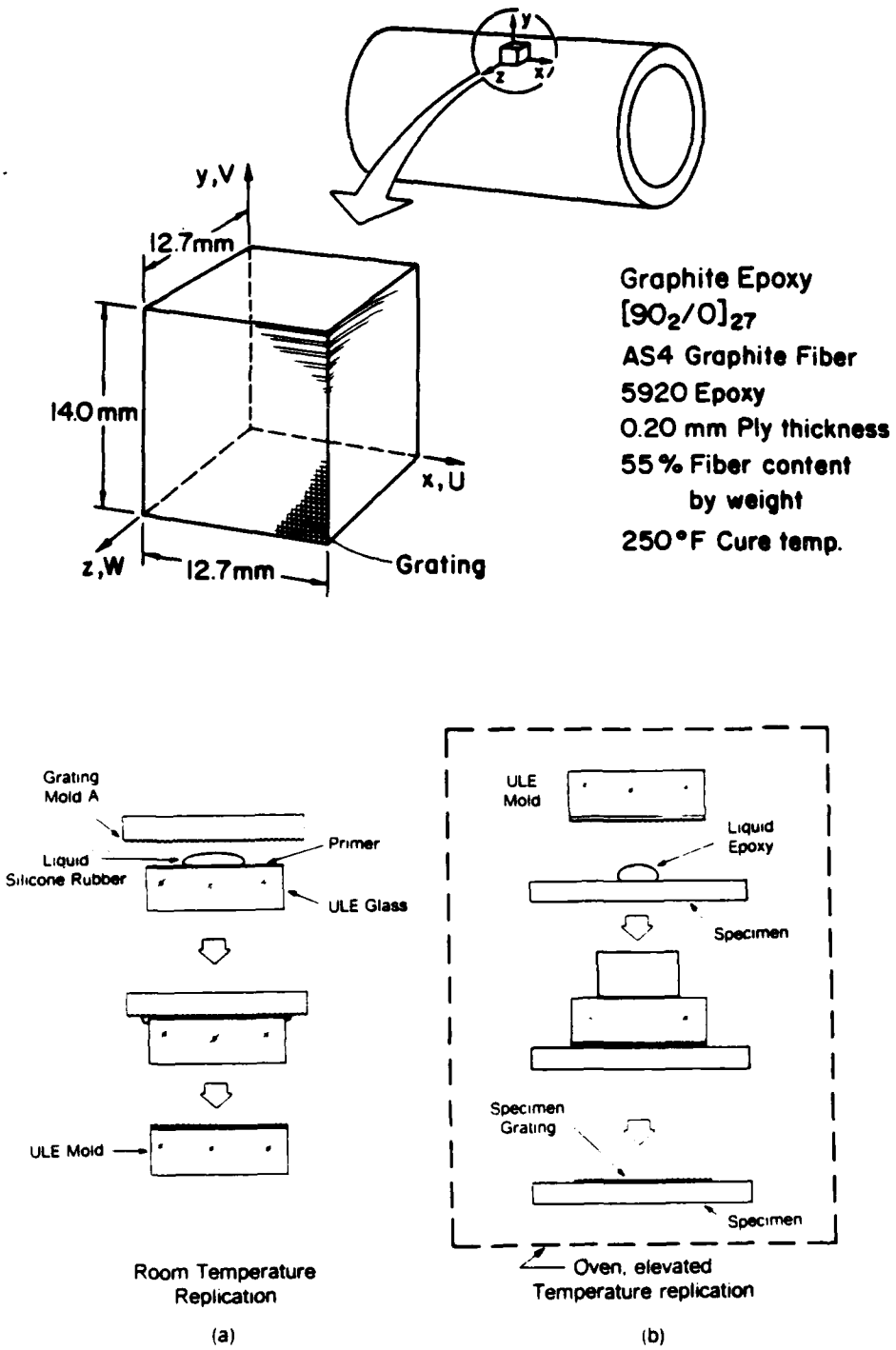

Fig. 20 Detail of the composite cube specimen for the residual thermal strain experiment. The procedure for the replication of the grating is shown schematically.

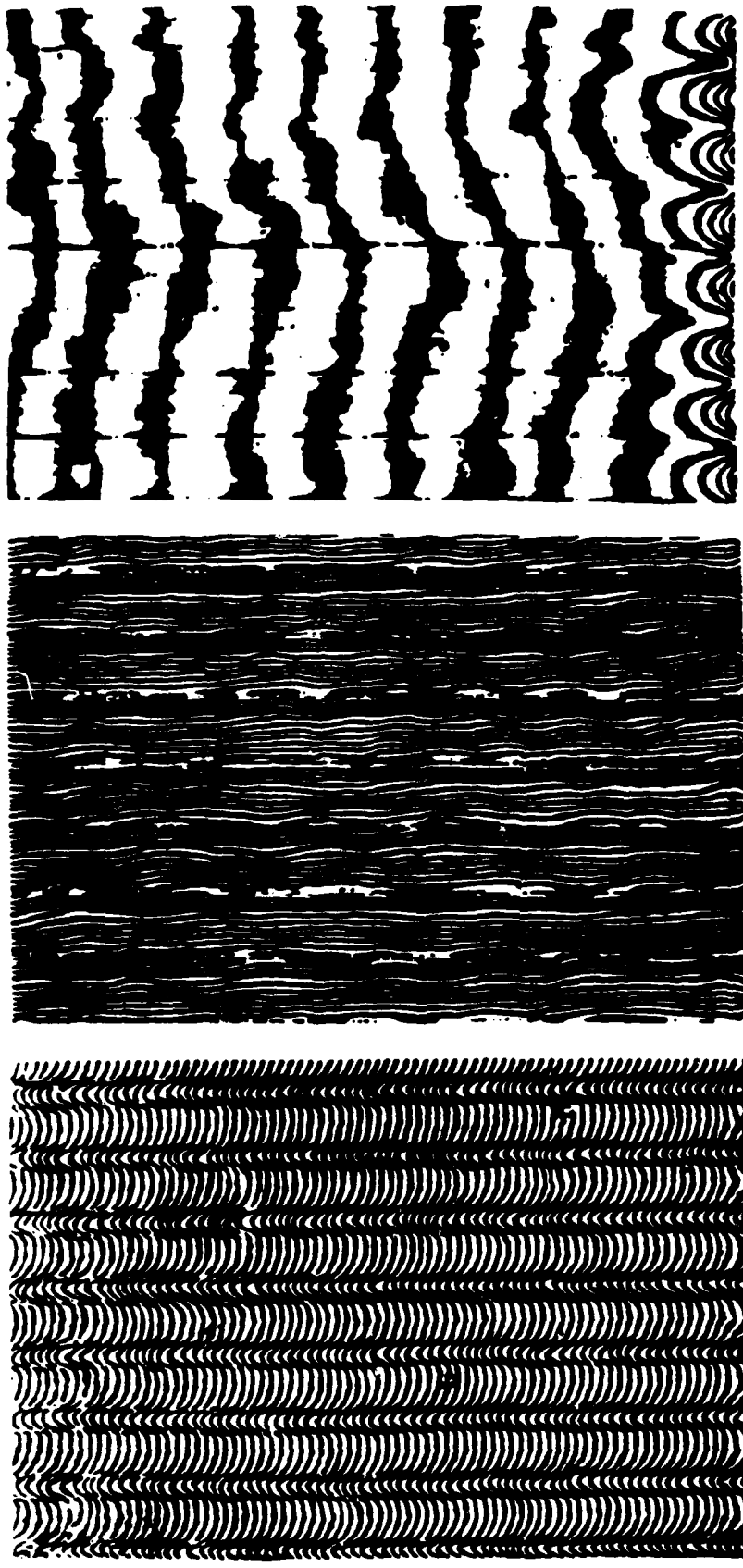

Fig. 21 Fringe patterns depictng residual thermal displacements contours (U, V and Z components) for the face of a composite cube.

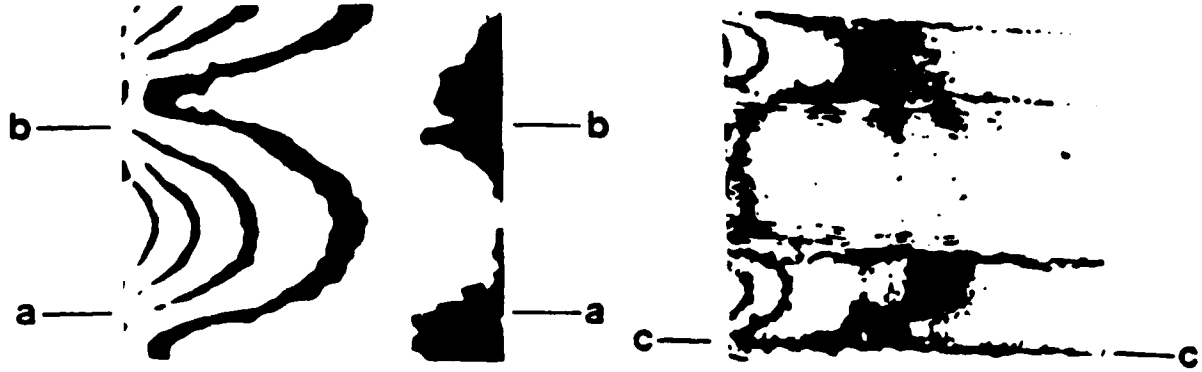

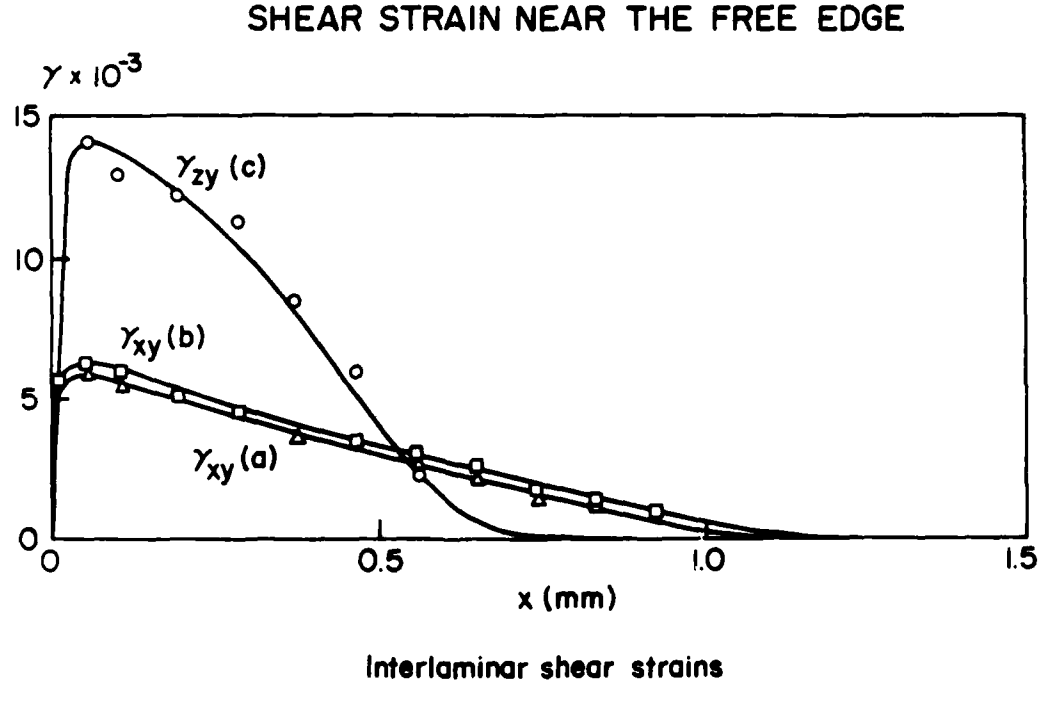

Fig. 22 Detail of (corner) edge effect displacement contours for the faces of the composite cube. Corresponding interlaminar shear strain distributions at ply interfaces are also shown.

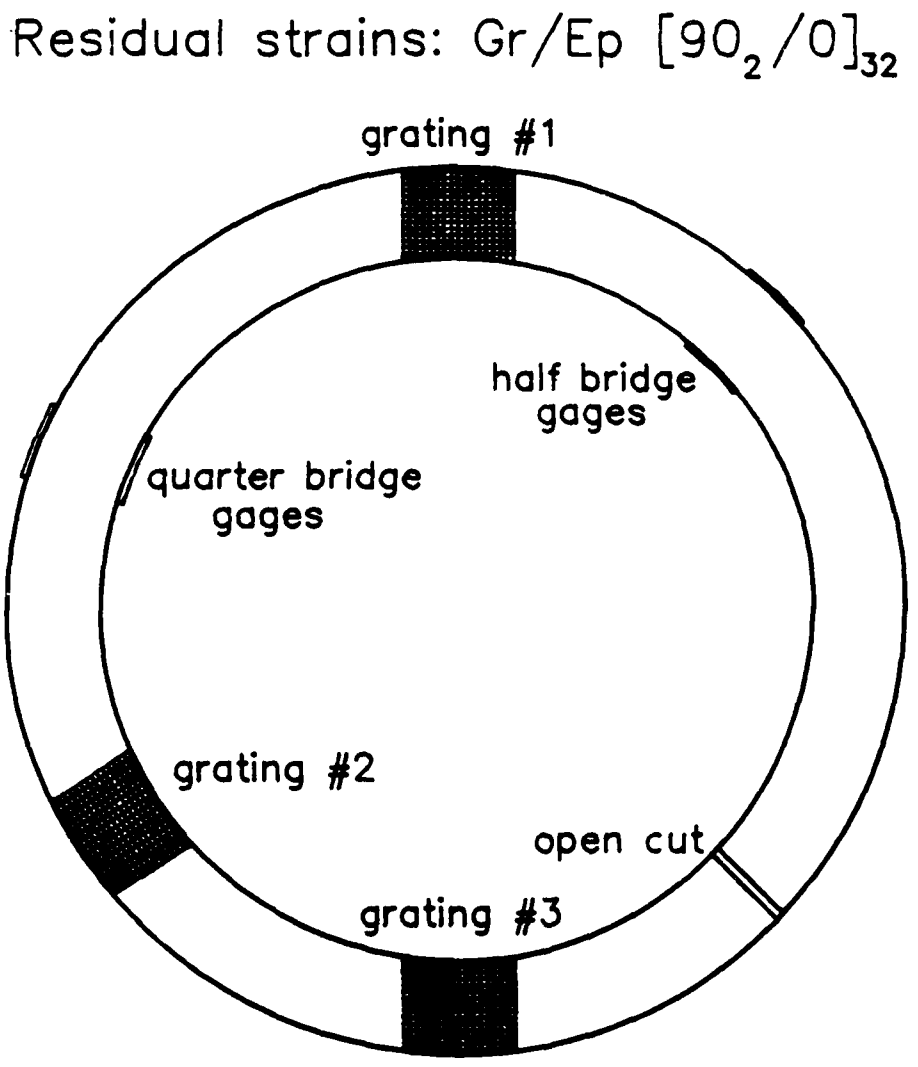

Fig. 23 Generally arrangement of moire gratings and strain gages on a thick-composite ring prior to cutting and measurement of residual mechanical strains.

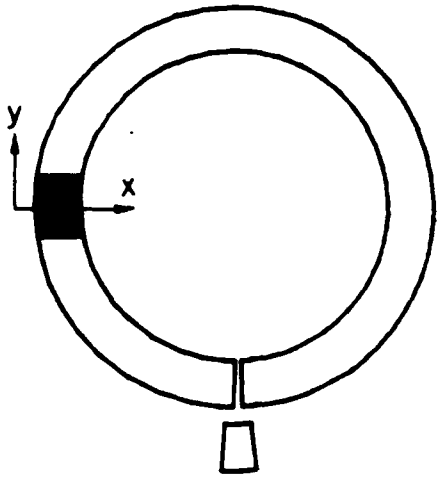

ϵ_y Relieved:

ID: $-730\,\mu\epsilon$

OD: $790\,\mu\epsilon$

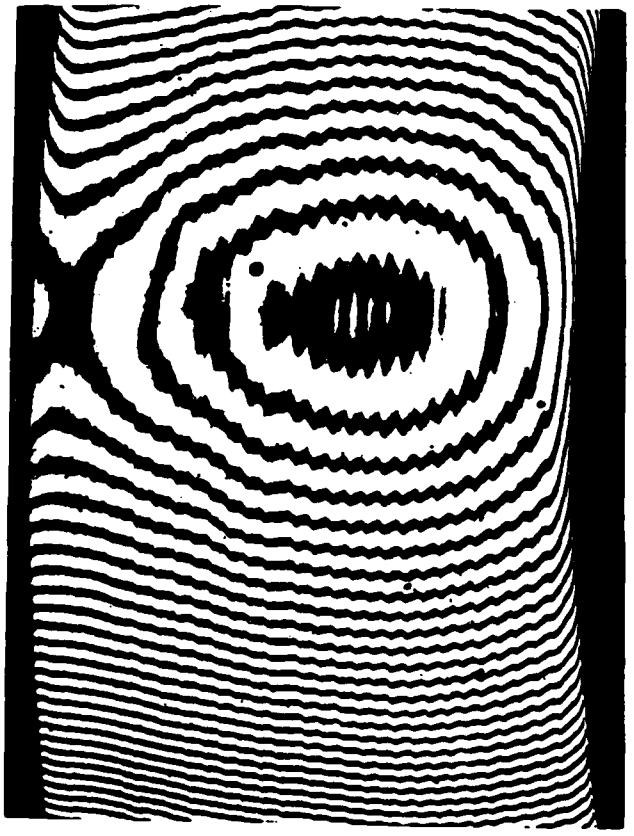

U

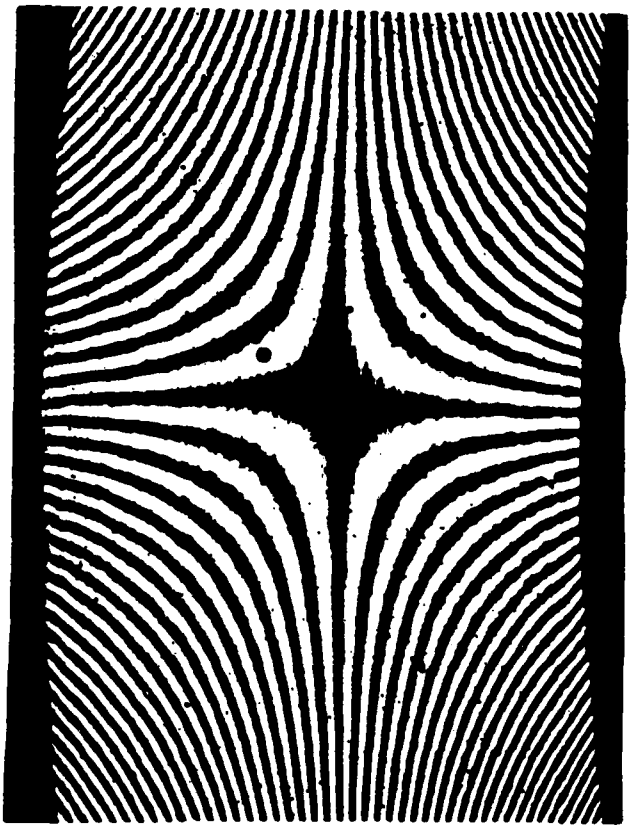

V

Fig. 24 Fringe patterns showing components of displacements relieved by a single through-cut.

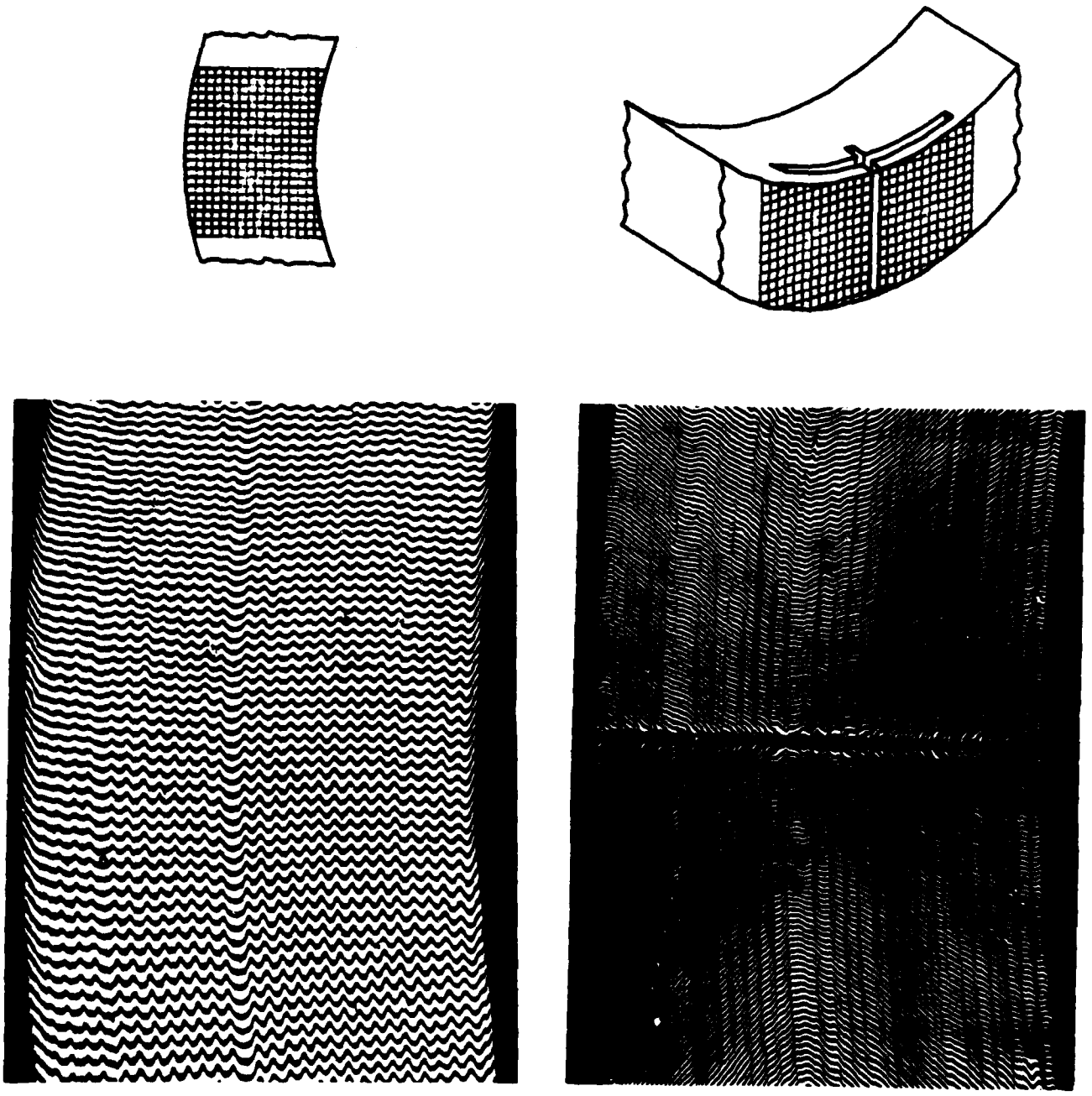

Fig. 25 Fringe patterns corresponding to out-of-plane displacements relieved by the through cut and local cuts.

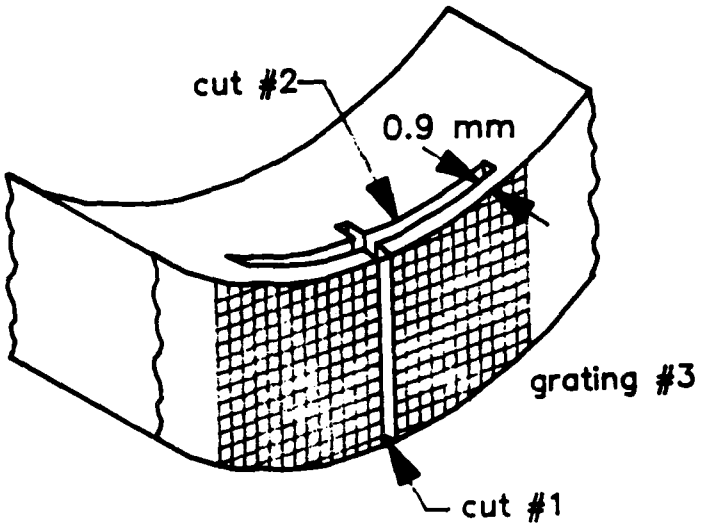

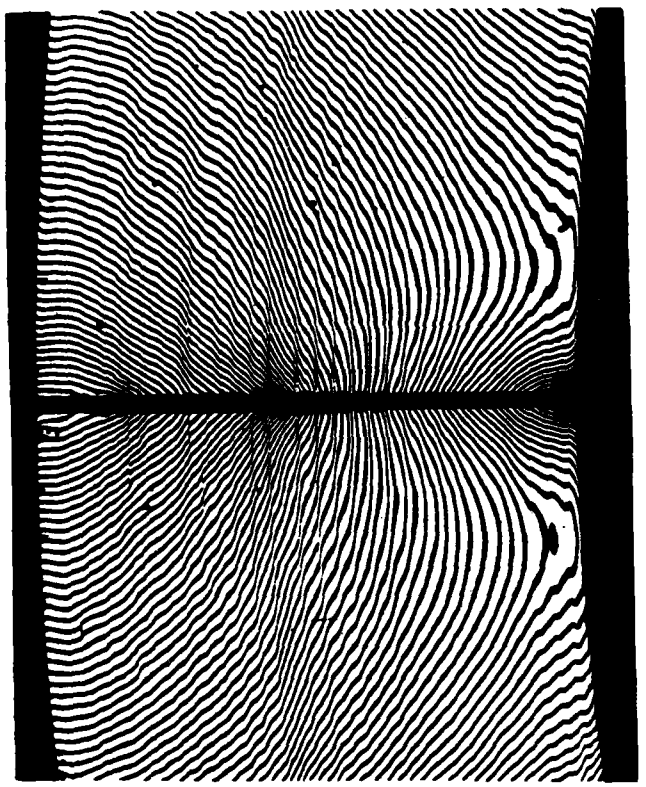

U

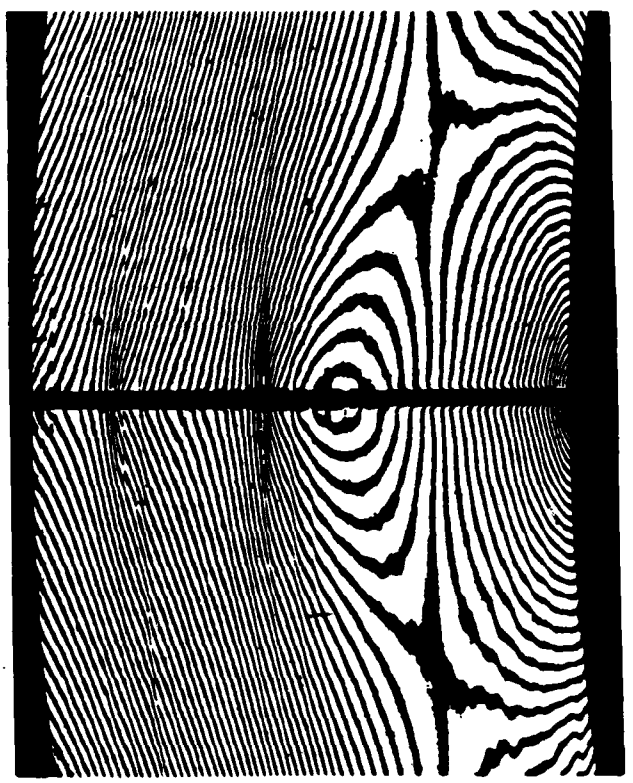

V

Fig. 26 Fringe patterns showing displacements relieved by additional, local, cutting.

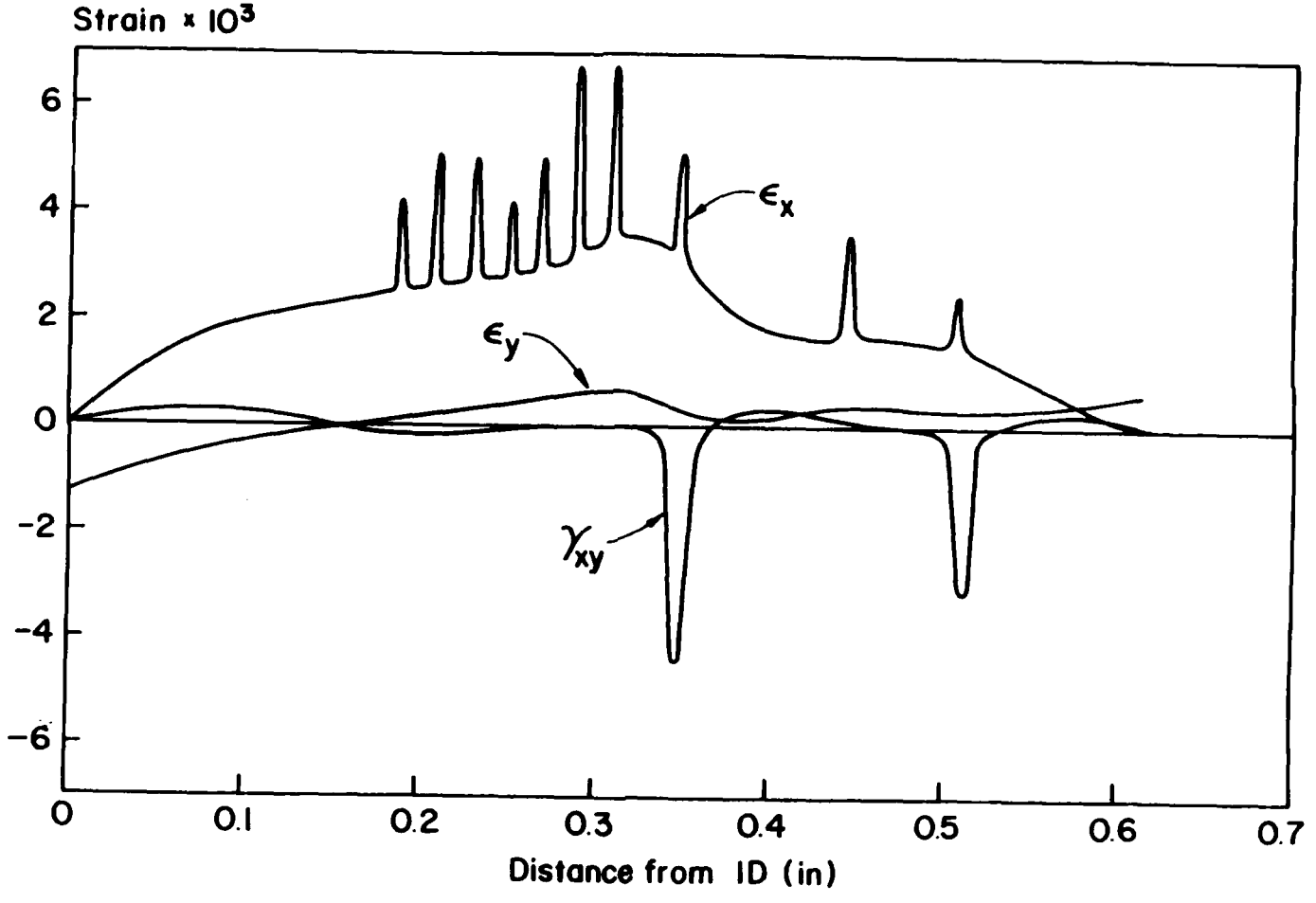

Fig. 27 Residual strain distributions for the thick composite ring. The peaks in γ_{xy} coincide with intermediate stages in curing and stacking errors.

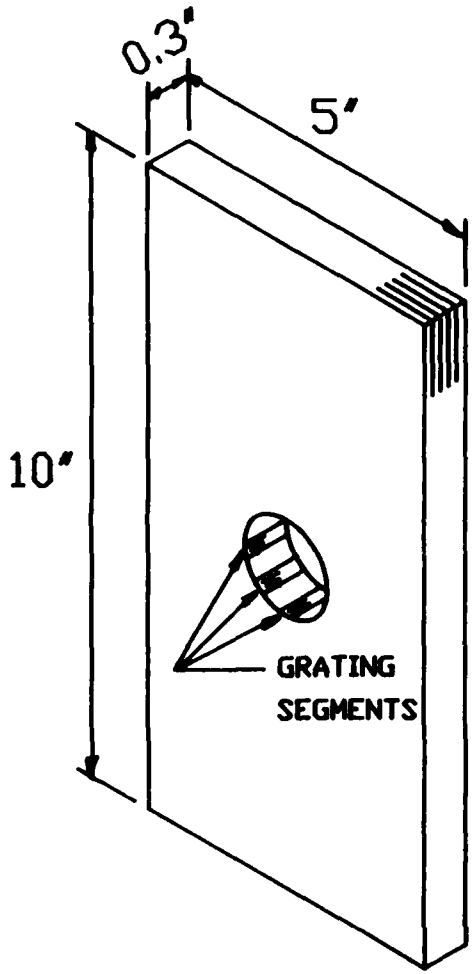

STACKING SEQUENCE

$[0_2/90]_{3S}$

$[0/45/90/-45/0]_{3S}$

HOLE SIZE

1" DIAMETER CIRCULAR HOLE

1" x 1-1/2" ELLIPTICAL HOLE

MAXIMUM LOAD

60,000 lbs. COMPRESSION

MATERIAL

GLASS/EPOXY

GRAPHITE/EPOXY

Fig. 28 Specimen configuration for edge effect studies in and around a cut out in a compression loaded composite panel.

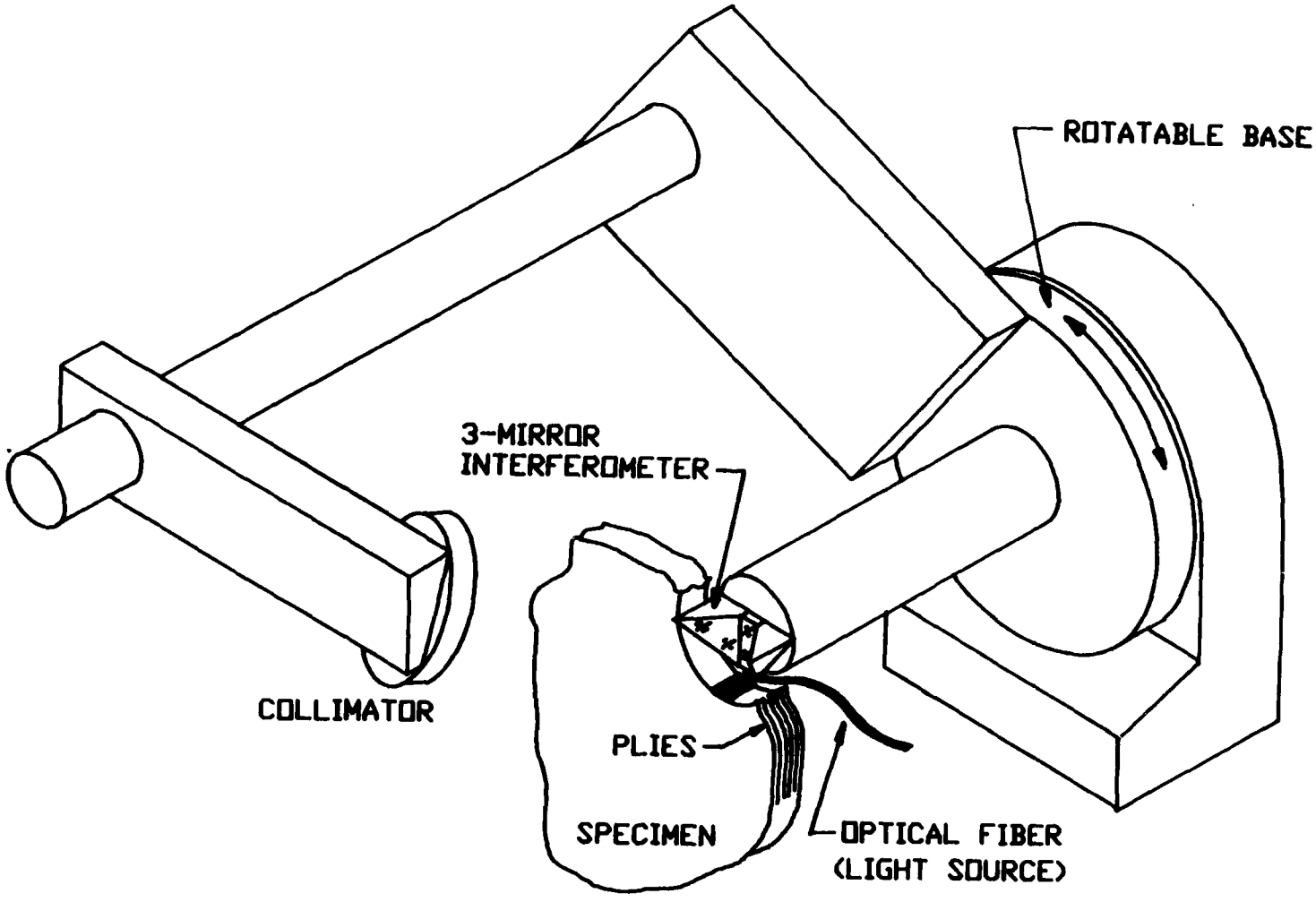

Fig. 29 General arrangement of the moire interferometer designed to interrogate the boundary surface of the hole in the compression panel program.

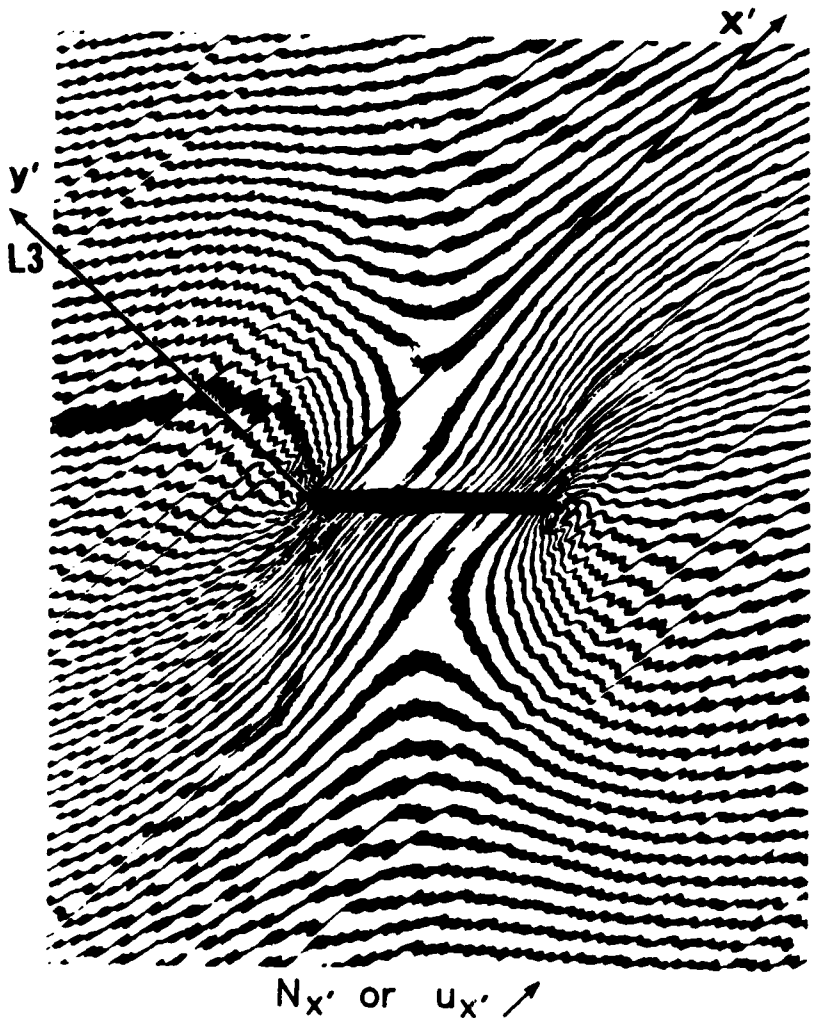

Fig. 30 Contour map of displacements parallel to 45° fiber direction in boron/aluminum laminate.

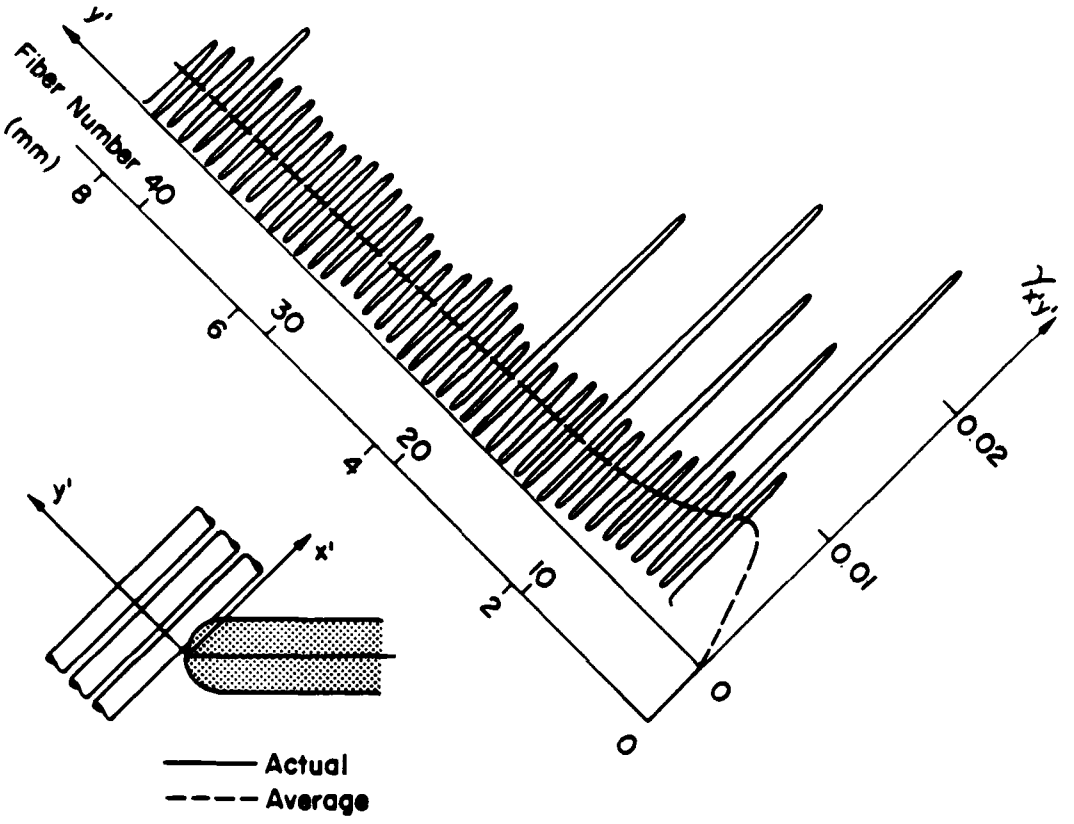

Fig. 31 Shear strains along line L3 (defined in Fig. 30).

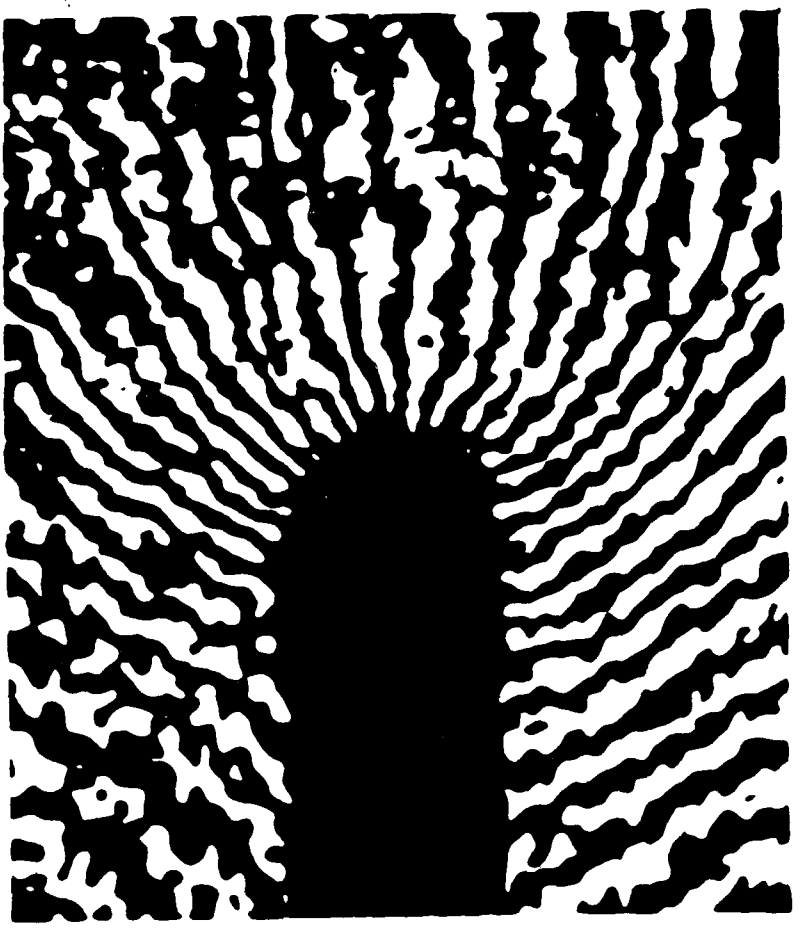

Fig. 32 Preliminary result of the ultrahigh sensitivity displacement measurement study. The fringes correspond to moire with about 500,000 lines per inch.

REPORT DOCUMENTATION PAGE

1a REPORT SECURITY CLASSIFICATION	1b RESTRICTIVE MARKINGS
2a SECURITY CLASSIFICATION AUTHORITY	3 DISTRIBUTION/AVAILABILITY OF REPORT
2b DECLASSIFICATION/DOWNGRADING SCHEDULE	
4 PERFORMING ORGANIZATION REPORT NUMBER(S)	5 MONITORING ORGANIZATION REPORT NUMBER(S)

6a NAME OF PERFORMING ORGANIZATION Virginia Polytechnic Institute and State University	6b OFFICE SYMBOL (If applicable) Blacksburg, VA	7a NAME OF MONITORING ORGANIZATION Office of Naval Research	
6c ADDRESS (City, State, and ZIP Code) 227 Norris Hall Engineering Science and Mechanics Dept. Blacksburg, VA 24061		7b ADDRESS (City, State, and ZIP Code) Mechanics Division (Code 430) 800 N. Quincy Street Arlington, VA 22217	
8a NAME OF FUNDING/SPONSORING ORGANIZATION Office of Naval Research	8b OFFICE SYMBOL (If applicable)	9 PROCUREMENT INSTRUMENT IDENTIFICATION NUMBER N00014-86-K-0255	
8c ADDRESS (City, State, and ZIP Code)		10 SOURCE OF FUNDING NUMBERS	
		PROGRAM ELEMENT NO	PROJECT NO / TASK NO / WORK UNIT ACCESSION NO

11 TITLE (Include Security Classification)
Phenomenological Studies in Micromechanics

12 PERSONAL AUTHOR(S)
D. Post and R. Czarnek

13a TYPE OF REPORT Final	13b TIME COVERED FROM _____ TO _____	14 DATE OF REPORT (Year, Month, Day) 1988-9-30	15 PAGE COUNT

16 SUPPLEMENTARY NOTATION

17 COSATI CODES		
FIELD	GROUP	SUB-GROUP

18 SUBJECT TERMS (Continue on reverse if necessary and identify by block number)
Micromechanics, Composites, interlaminar, displacement fields, strains, moire interferometry, diffraction gratings, experimental methods.

19 ABSTRACT (Continue on reverse if necessary and identify by block number)

see attached sheet

20 DISTRIBUTION/AVAILABILITY OF ABSTRACT ☒ UNCLASSIFIED/UNLIMITED ☐ SAME AS RPT ☐ DTIC USERS	21 ABSTRACT SECURITY CLASSIFICATION
22a NAME OF RESPONSIBLE INDIVIDUAL	22b TELEPHONE (Include Area Code) / 22c OFFICE SYMBOL

DD FORM 1473, 84 MAR — 83 APR edition may be used until exhausted. All other editions are obsolete.

SECURITY CLASSIFICATION OF THIS PAGE

19. ABSTRACT

State of the art experimental techniques have been applied to micromechanical measurements of advanced composite materials and structures.

Moire interferometry has been used to determine the phenomenological nature of deformation of thick graphite epoxy laminates, and to measure representative mechanical properties. These properties include Young's modulus, Poisson's ratios, shear moduli and co-efficients of thermal expansion.

Test methods used for the measurement of shear moduli have been evaluated and a new test configuration proposed.

The photomechanics experiments uncovered and quantified edge effects which were also studied in detail numerically. The practical nature of stresses, which are held in some circles to be singular, was investigated and the scale over which these effects act was determined. It would appear that a very fine scale and extremely high local stress gradients occur.

A micromechanical analysis of metal-matrix specimens revealed highly anomalous deformations.

A series of experiments has been performed to determine the magnitude and distribution of residual stresses in thick composites. The experiments were particularly successful in uncovering highly localized residual tensile and shear strain concentrations.

Many of the experimental observations were made possible by the expansion of laboratory facilities which were completed towards the middle of this reporting period. This expansion has allowed significant developments in the techniques of high sensitivity strain measurement. Improvements in grating quality have been achieved and applied to composite mechanics investigations. Experiments have been taken off the optical table and performed on a universal testing machine. A two stage process to yield an almost ten-fold increase in sensitivity has been investigated; preliminary results are exciting. This method will allow further penetration into the micromechanics domain in composite materials. Complementing this research, significant progress toward achieving zero-thickness gratings has been made.

A very active research group which includes three faculty and seven Ph.D. students has been established and many research papers are in preparation.